Multi-way modelling of oral microbial dynamics and host-microbiome interactions during induced gingivitis

G.R. van der Ploeg[1], B.W. Brandt[2], B.J.F. Keijser[3], M.H. van der Veen[2,4], C.M.C. Volgenant[2,5], E. Zaura[2], A.K. Smilde[1], J.A. Westerhuis[1], A. Heintz-Buschart[1*]

[1] *Biosystems Data Analysis, Swammerdam Institute for Life Sciences, University of Amsterdam, Amsterdam, The Netherlands*

[2] *Preventive Dentistry, Academic Centre for Dentistry, Vrije Universiteit Amsterdam and University of Amsterdam, Amsterdam, The Netherlands*

[3] *Microbiology and Systems Biology, TNO Healthy Living and Work, Leiden, The Netherlands*

[4] *Paediatric Dentistry, Academic Centre for Dentistry, Vrije Universiteit Amsterdam and University of Amsterdam, Amsterdam, The Netherlands*

[5] *Cariology, Academic Centre for Dentistry, Vrije Universiteit Amsterdam and University of Amsterdam, Amsterdam, The Netherlands*

*Author for correspondence: Anna Heintz-Buschart a.u.s.heintzbuschart@uva.nl

Geert Roelof van der Ploeg:	https://orcid.org/0009-0007-5204-3386
Monique van der Veen:	https://orcid.org/0000-0002-6844-4682
Bart Keijser:	https://orcid.org/0000-0003-1597-2948
Catherine Volgenant:	https://orcid.org/0000-0002-4049-2914
Bernd Brandt:	https://orcid.org/0000-0002-1155-1989
Egija Zaura:	https://orcid.org/0000-0003-1432-6194
Age Smilde:	https://orcid.org/0000-0002-3052-4644
Johan Westerhuis:	https://orcid.org/0000-0002-6747-9779
Anna Heintz-Buschart:	https://orcid.org/0000-0002-9780-1933

Abstract

Gingivitis - the inflammation of the gums - is a reversible stage of periodontal disease. It is caused by dental plaque formation due to poor oral hygiene. However, gingivitis susceptibility involves a complex set of interactions between the oral microbiome, oral metabolome and the host. In this

study, we investigated the dynamics of the oral microbiome and its interactions with the salivary metabolome during experimental gingivitis in a cohort of 41 systemically healthy participants. We use Parallel Factor Analysis (PARAFAC), which is a multi-way generalization of Principal Component Analysis (PCA) that can model the variability in the response due to subjects, variables and time. Using the modelled responses, we identified microbial subcommunities with similar dynamics that connect to the magnitude of the gingivitis response. By performing high level integration of the predicted metabolic functions of the microbiome and salivary metabolome, we identified pathways of interest that describe the changing proportions of Gram-positive and Gram-negative microbiota, variation in anaerobic bacteria, biofilm formation and virulence.

Key Words

Longitudinal data, Salivary metabolomics, Parallel Factor Analysis, Data integration, Pathway enrichment analysis

Introduction

Microbial oral diseases, such as dental caries and gum inflammation, are a global public health burden (Peres et al., 2019; Petersen et al., 2005; WHO, 2022). Together, they are the most prevalent health condition world-wide, impacting quality of life and imposing a significant economic burden with 5-10% of public health expenditure in most industrialized countries (WHO, 2022; Widström et al., 2004). Prevention of oral diseases is therefore of critical importance.

Gingivitis is a reversible stage of periodontal disease marked by inflamed, bleeding gums (Chapple et al., 2015; Curtis et al., 2020; Huang et al., 2014). It is caused by dental plaque accumulation due to poor oral hygiene (Löe et al., 1965; Murakami et al., 2018) and is present in a substantial part of the global population (Han et al., 2020; WHO, 2022). The pathogenesis of gingivitis involves a complex set of interactions between the oral microbiome, the oral metabolome and the host (Chapple et al., 2018; Huang et al., 2014). These are in turn dependent on many factors (Chapple et al., 2018; Kilian et al., 2016), including host diet (Van Der Velden et al., 2011), life-style (Bergström & Preber, 1986), and genetics (Nibali et al., 2017). Therefore, the oral microbiome alone does not determine whether and to what extent gingivitis develops, as can be seen by the high degree of individual variation in gingivitis susceptibility seen in experimental gingivitis models after refraining from toothbrushing (Axelsson et al., 1991; Chapple et al., 2015, 2018; Guk et al., 2020; Huang et al., 2014; van der Veen et al., 2016)

While there is no monocausal microbial agent in gingivitis, the gingival crevice microbiota underneath the gums shifts to a dysbiotic state (Abusleme et al., 2021; Curtis et al., 2020; Diaz et al., 2016). The depletion of Gram-positive bacteria, such as *Rothia dentocariosa,* and enrichment in Gram-negative bacteria such as *Porphyromonas gingivalis*, *Prevotella* spp. and *Selenomonas* spp. is frequently observed in case-control comparisons, despite this shift being less pronounced compared to periodontitis progression (Curtis et al., 2020; Huang et al., 2014; Kistler et al., 2013; Schincaglia et al., 2017). Additionally, increasing subgingival anaerobiosis during gingivitis progression promotes the growth of pathobionts (Curtis et al., 2020; Diaz et al., 2002; Ter Steeg et al., 1988).

Being the medium through which the host and the microbiota interact, the salivary metabolome is often studied as a non-invasive diagnostic of oral disease (Dawes & Wong, 2019; Proctor, 2016). A well-known host-microbiome interaction is the relation between host sugar consumption and the production of acids by the dental plaque microbiota. This lowers the local pH and shifts the microbiota further towards dysbiosis (König & Navia, 1995; Marsh, 1991). However, many other dynamic microbe-microbe and host-microbiome interactions that occur throughout gingivitis onset and progression are not well understood.

Here, we investigate the spatially resolved oral bacterial microbiome and its interactions with the salivary metabolome during experimental gingivitis to (1) identify microbial subcommunities with common dynamics and (2) pinpoint potential impacts on biochemical pathways. Reversible gingivitis was induced in a cohort of 41 systemically healthy participants by omission of oral hygiene during a two-week gingivitis challenge (**Figure 1A**; (Prodan et al., 2016; van der Veen et al., 2016)). Previously reported plaque levels, gingival bleeding upon probing, and red fluorescent plaque quantification allowed grouping of the participants into identified low, mid and high responders based on the last day of the intervention (**Figure 1B**; (van der Veen et al., 2016)). During a two-week baseline period at two time points (day -14 and day 0), a challenge period at four time points (day 2 to day 14), and one week resolution period at one time point (day 21), the oral microbiome was determined at six sites: tongue, saliva, supragingival plaque at the lower and upper lingual surfaces and supragingival plaque at the lower and upper interproximal surfaces (**Figure 1C**). To identify the individual variation in the time-resolved response of the oral microbiome to the challenge and describe commonly responding (groups of) microbiota, we employ Parallel Factor Analysis (PARAFAC; (Carroll & Chang, 1970; Harshman, 1970)), for modelling the subjects, time, and microbial abundances at each site (**Figure 1D**). The salivary metabolome dynamics, assessed in

unstimulated saliva during the challenge, is likewise modelled and integrated with microbiome models at the biochemical pathway level. These analyses should yield insights into microbial processes that underlie individual gingivitis responses.

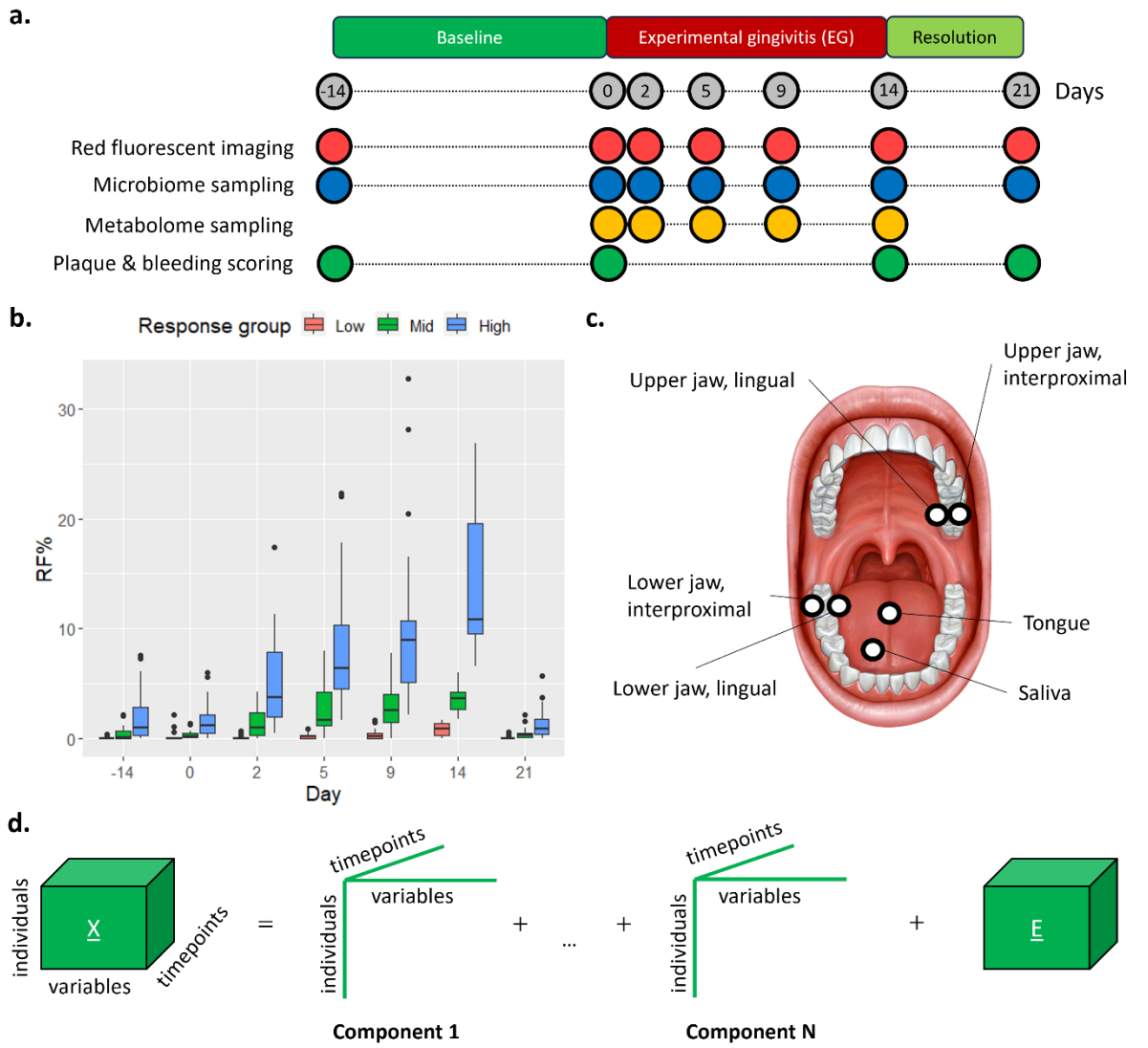

Figure 1: Overview of the study design and analysis. (a) Timeline of experimental gingivitis challenge with analyses; (b) gingivitis responses: Three groups of responders were identified based on red fluorescent dental plaque (RF%) at day 14: low (0-1.7%), mid (1.8-6.0%) and high (6.0%+); (c) oral sampling sites; (d) data analysis approach: Parallel factor analysis (PARAFAC), a multi-way generalization of Principal Component analysis, decomposes a multi-way data cube into components with three loading vectors each: one for the subjects, one for the variables (here: microbial relative abundances) and one for time. This approach allows us to identify the individual variation in the time-resolved response to the challenge and to describe commonly responding groups of microbiota.

Results

PARAFAC describes clinically relevant variation in oral microbiomes between subjects

To describe the microbial dynamics of each oral site for all subjects across time, we analysed 16S rRNA gene amplicon sequencing data for a total of 14,014 amplicon sequence variants (ASVs). After removal of sparse ASVs, we created separate PARAFAC models for each oral site, choosing the most appropriate number of PARAFAC components by inspecting the number of iterations needed to converge (Bro, 1997), the core consistency diagnostic (Bro & Kiers, 2003), the variation explained (Bro, 1997), and the tucker congruence coefficient per mode (Lorenzo-Seva & ten Berge, 2006; Tucker, 1951) (**Supplementary Data**). This yielded two-component models for the upper jaw lingual plaque (19.7% explained variation) and upper jaw interproximal plaque (16.5%), tongue (31.5%) and saliva (17.5%) microbiomes (**Figure 2**). Lower jaw lingual and interproximal plaque microbiomes were best represented by one-component models (explaining 11.4% and 7.2% of the variation, respectively). The model of the lower jaw interproximal plaque microbiome was not investigated further due to the limited amount of explained variation and due to the model not describing biologically meaningful information.

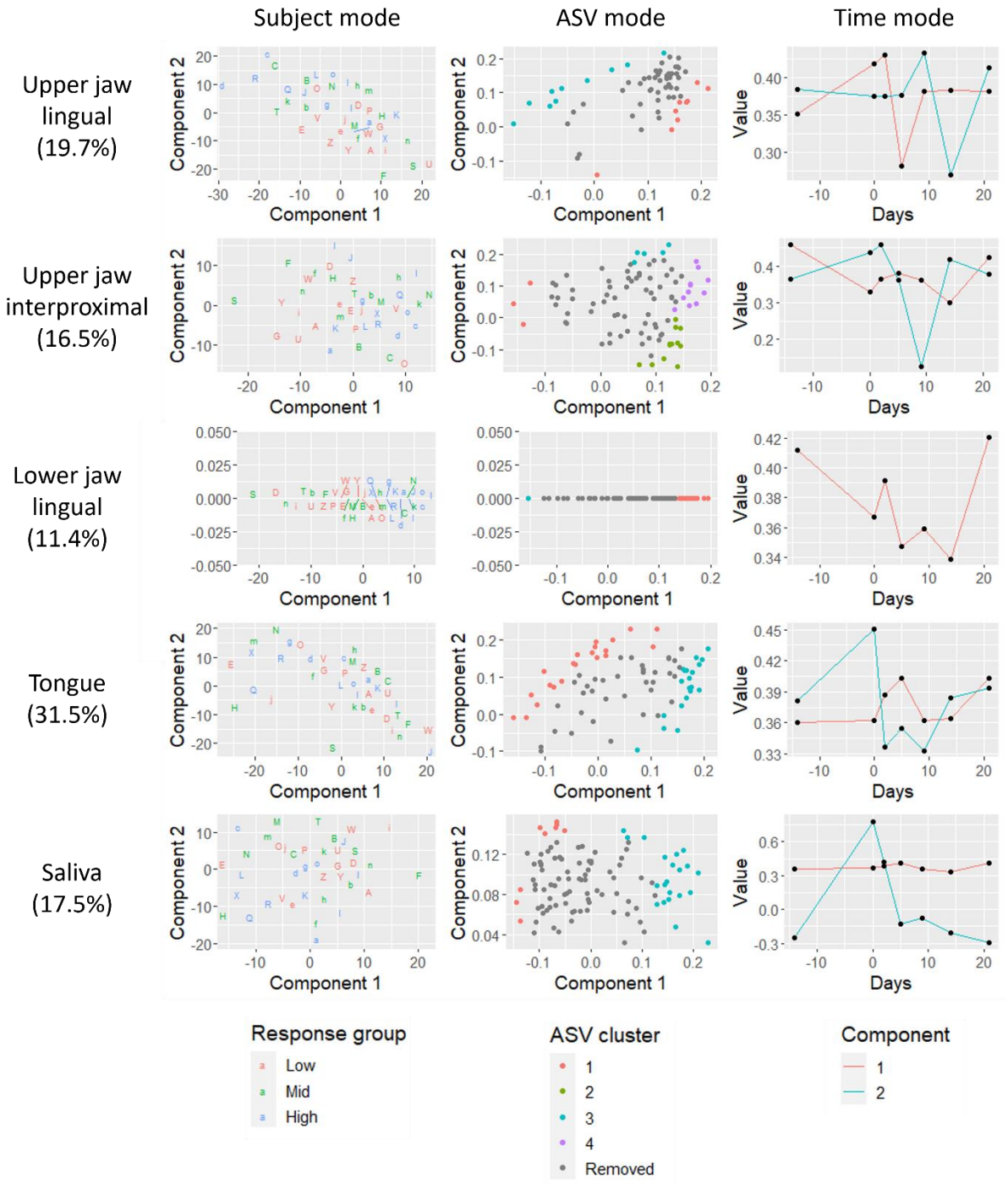

*Figure 2: Overview of the PARAFAC models per sample type. In the rows, the PARAFAC models per sample type are described: upper jaw lingual plaque, upper jaw interproximal plaque, lower jaw lingual plaque, tongue and saliva. Variance explained per model are shown in the sample type labels. In the left column the loadings of the first and second component in the subject mode are plotted against each other, with every subject having a unique character to identify them across the sample types. In the middle column the loadings of the first and second component in the ASV mode are plotted against each other. We identified microbial subcommunities (ASV clusters) with common responses per sampling site by selecting and then clustering well-modelled ASVs based on their fitted response (Methods, **Table 2**). ASVs are color-coded by cluster number (or shown in grey if removed prior to clustering). In the right column, the loadings per time point are shown per component. The model corresponding to the lower jaw lingual plaque only has one component. The model of the lower jaw interproximal plaque microbiome was not investigated further due to the limited amount of explained variation and due to the model not describing biologically meaningful information.*

132 To interpret the models, we tested the correlation between the time-resolved subject loadings of
133 each component with the measured parameters of gingivitis. This approach revealed correlation of
134 components with one or more clinical parameter for the three plaque microbiomes (**Table 1**).
135 Overall, the PARAFAC models describe the variation that exists between subjects, rather than the
136 variation within a subject (one-sided Wilcoxon rank-sum test: p=0.020, **Supplementary Figures A1**
137 **and A2**). Furthermore, subject age was found to be significantly described by the first component of
138 the model corresponding to the tongue microbiome samples (p=0.035) and the second component
139 of the model corresponding to the saliva microbiome samples (p=0.038) (**Supplementary Table B1**).
140 Gender was not significantly described by any model (**Supplementary Table B1**). We also performed
141 Pearson correlation tests of the time-resolved subject loadings per component with richness and
142 evenness. All microbiome models were found to contain at least one component that significantly
143 described richness or evenness ($p \leq 0.05$; **Table 1**). In conclusion, the PARAFAC models represented
144 clinically and ecologically relevant parameters.

145 *PARAFAC describes microbial subcommunities with common gingivitis responses*

146 Building on the interpretability of the subject modes (**Table 1**), we identified microbial
147 subcommunities with common responses per sampling site by selecting and then clustering well-
148 modelled ASVs based on their fitted response (**Figure 2**, for cluster membership see **Table 2**). Per
149 sampling site, at least one subcommunity containing mainly pathobionts or pro-inflammatory
150 genera such as *Actinomyces*, *Campylobacter*, *Capnocytophaga*, *Fusobacterium*, *Leptotrichia* and
151 *Porphyromonas* (Huang et al., 2014; Kirst et al., 2015; Kistler et al., 2013; Schincaglia et al., 2017;
152 The Human Microbiome Project Consortium, 2012) and one subcommunity containing mainly
153 commensal genera such as *Kingella oralis* (Abusleme et al., 2021), *Streptococcus* spp. (Caporaso et
154 al., 2011; Zaura et al., 2009), and *Veillonella* spp. (Moore & Moore, 1994) have been identified.

155 The sum of the relative abundances of the ASVs in each cluster was determined to test the difference
156 between the microbiomes of individuals in the low and high response groups at every time point
157 per oral site (Benjamini-Hochberg corrected permutation test of mean difference: $p \leq 0.05$;
158 **Supplementary Table B2)**. This approach revealed significant differences in the relative abundance
159 of most plaque-associated ASV clusters in high responders compared to the low responders at
160 baseline (day -14; **Figure 3**, **Supplementary Figure A3**). As such, the PARAFAC models of plaque
161 microbiomes describe microbial subcommunities with common dynamics that connect to the
162 magnitude of the gingivitis response.

We further investigated the robustness of the ecosystem during gingivitis onset and progression by comparing the sum of the relative abundances per cluster at the start and end of the intervention (**Supplementary Table B3**). We found significant differences between the relative abundances of some ASV clusters at the start and end of the gingivitis challenge in lower jaw lingual (ASV cluster 1) and upper jaw interproximal (ASV cluster 4) plaque microbiomes in all response groups (Benjamini-Hochberg corrected two-sided Wilcoxon rank sum test: $p \leq 7.2e-13$ and $p \leq 2.6e-6$, respectively). For a further three ASV clusters (upper jaw lingual ASV cluster 1 and upper jaw interproximal clusters 1 and 3), we found the sum of relative abundances to be significantly different ($p=0.002$, $p=0.0025$, $p=0.0039$, respectively) in high responders, but not in low responders. These results suggest that ecosystem stability is different between high and low responders in several oral niches.

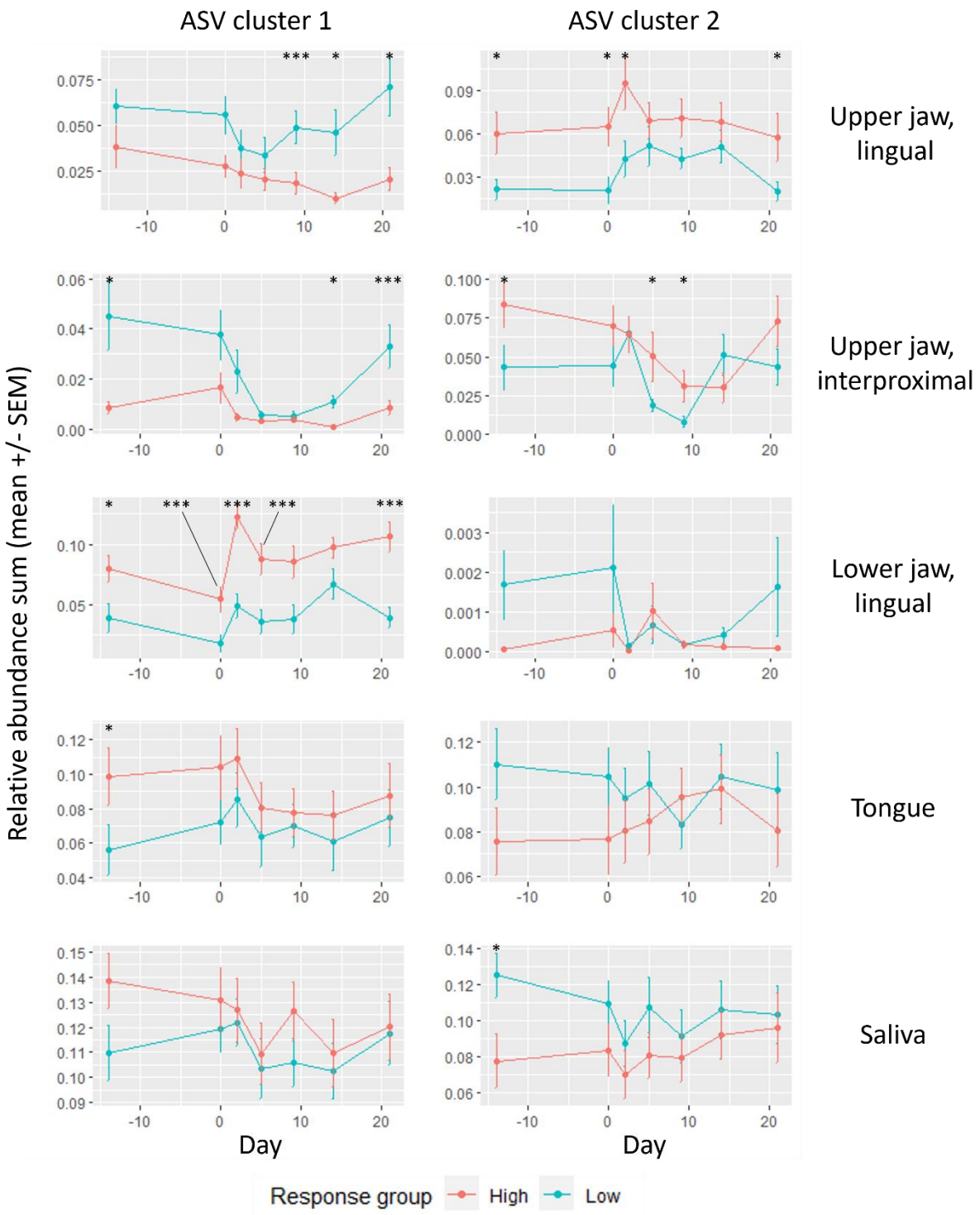

Figure 3: Overview of the sums of relative abundances per ASV cluster and sample type, separating subjects by response group. Error bars correspond to the standard error of the mean (SEM). The mean difference between the high and low response groups per time point was tested using a Benjamini-Hochberg corrected permutation test of 999 iterations (: p≤0.05; **: p≤0.01; ***: p≤0.001). Mid responders and ASV clusters 3 and 4 of the upper jaw interproximal plaque samples are not shown for visual clarity (**Supplementary Figure A3** and **A4**, respectively). Please refer to **Table 2** for the list of identified species per ASV cluster.*

182 *Integration of the microbiome and metabolome PARAFAC models identifies host-microbiome*
183 *interactions at the pathway level*

184 With the established connection between the clinical parameters of gingivitis and the variation in
185 the plaque microbiomes as modelled by PARAFAC, we investigated host-microbiome interactions
186 at the biochemical pathway level. We obtained functional predictions of the microbiome per oral
187 site using Tax4Fun2 (Aßhauer et al., 2015; Wemheuer et al., 2020). We then created separate
188 PARAFAC models of the salivary metabolomics data and of the functional prediction of the
189 microbiomes at each oral site. Despite correcting for correlation between most salivary metabolite
190 levels, likely due to variable water content of the saliva (see Methods), the subject loadings of both
191 components of the model corresponding to the salivary metabolome were found to correlate with
192 the correcting factor (p=2.0e-14 and p=2.0e-5, respectively). Regardless, we expected the salivary
193 metabolomics model to have sufficient freedom to also describe variation related to the gingivitis
194 response.

195 The well-modelled molecular functions (KEGG orthologous groups belonging to pathways that
196 produce or consume the salivary metabolites) and well-modelled salivary metabolites were
197 combined in a ranked list. KEGG-pathway enrichment was identified using SetRank, which is a
198 functional enrichment algorithm that corrects for multiple pathway membership (Simillion et al.,
199 2017). This revealed that the microbiome and metabolome responses to the gingivitis challenge
200 reflected differences in carbon and energy metabolism, as well as cell wall structure (**Figure 4,**
201 **Supplementary Figure A5, Supplementary Table B4**). For example, the tongue microbiome and
202 salivary metabolome were involved in a joint response in the biosynthesis of cofactors and carbon
203 metabolism (p=0.0045 and p=0.0052, respectively). The quorum sensing pathway was significantly
204 enriched in all plaque microbiomes ($p \leq 0.05$). The pathway enrichment results therefore reflect the
205 microbiome responses and highlight potential metabolic interactions with the human host.

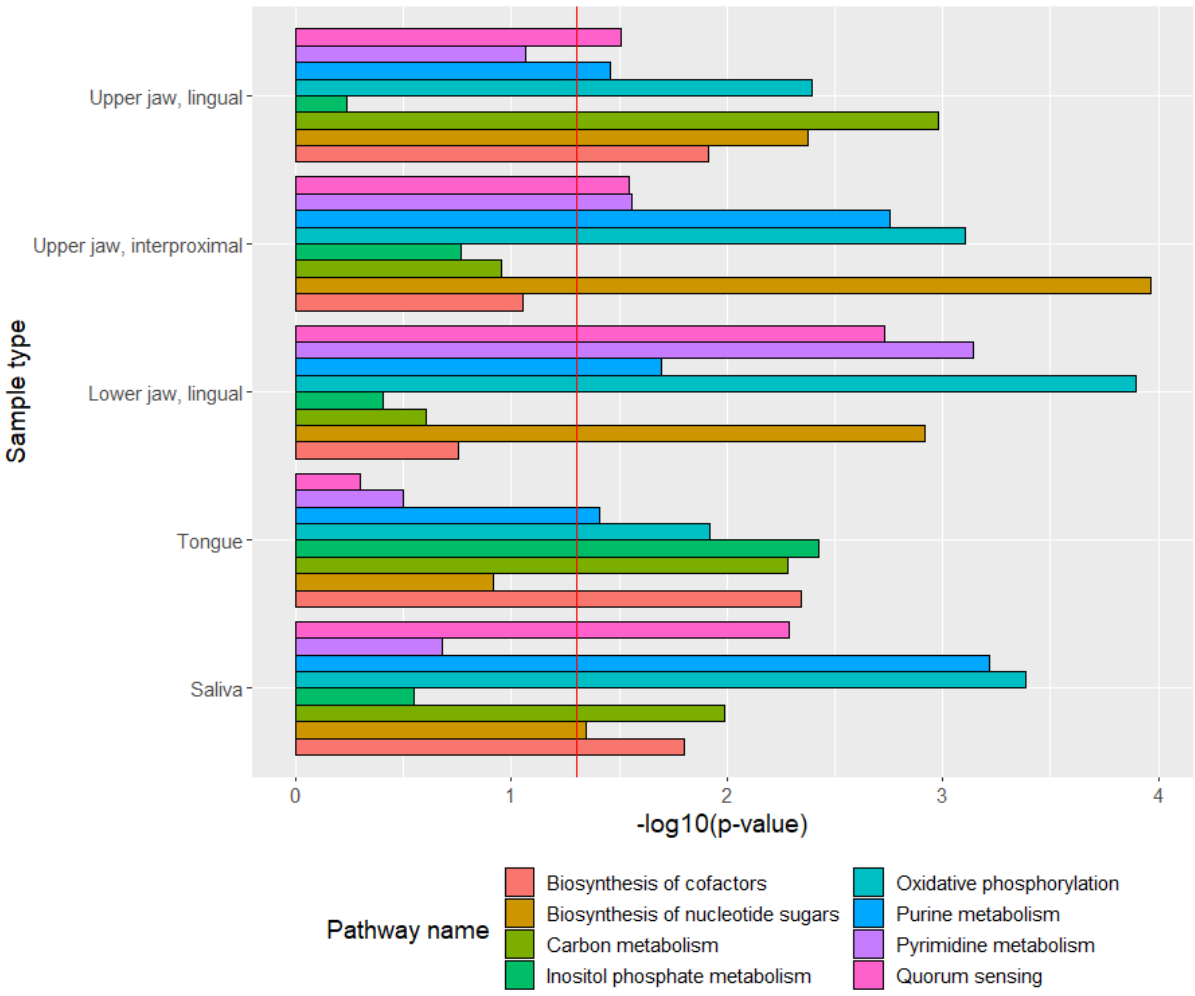

206

207 *Figure 4: Overview of the pathway enrichment results per combination of oral site microbiome and the salivary metabolome.*
208 *Tax4Fun2 was used to create functional predictions from ASV data. Well-modelled metabolites and microbiome molecular*
209 *functions were integrated by mapping them to KEGG pathway level. SetRank was then used to test for pathway enrichment*
210 *and corrected for multiple-pathway membership. Pathways were filtered to be significant (p<=0.01) in at least one sample*
211 *type and to contain at least two well-modelled KEGG molecular functions and two well-modelled metabolites. The red vertical*
212 *line corresponds to p=0.05.*

213

Discussion

We have shown that the unsupervised modelling approach of PARAFAC mainly described variation between subjects, as expected from an algorithm describing the maximum amount of variation that is present in the data. The modelled variation could be attributed to clinically relevant parameters. In addition, we have observed that the model corresponding to the salivary metabolomics samples partly describes the salivary dilution despite correcting for it using Probabilistic Quotient Normalization (Dieterle et al., 2006). This might be an artifact due to an incorrect assumption that correcting for water content of saliva can be done in the same way as for urine metabolomics samples. Future work on this topic should focus on the appropriateness of using Probabilistic Quotient Normalization prior to performing a decomposition analysis. Other multi-way approaches exist to describe a specific type of variation (Bro, 1997; Carroll & Chang, 1970; Harshman, 1970). For example, in N-way partial least squares (NPLS) the model is constrained to regress on an outcome variable (Bro, 1996). Additionally, the PARAFAC models of the microbiome and metabolome could be created in a linked fashion by keeping one of the modes equal to each other, known as coupled matrix and tensor factorization (Acar et al., 2014, 2015; Singh & Gordon, 2008). Each of these approaches might yield new insights as the models explicitly look at variation that is common between the datasets. Further research is needed to compare such methods to PARAFAC in the context of multi-omics data.

We observed that the microbiome PARAFAC models partly describe richness and evenness. This result gives further evidence of a relationship between oral health and microbial diversity which has been described before (Anderson et al., 2018; Schoilew et al., 2019; Thomas et al., 2014). While the methodology used in this study targeted only bacteria, while other members of the oral microbiome – such as viruses and fungi – might also be relevant in gingivitis onset and progression (Baker et al., 2017; Nobbs & Jenkinson, 2015). We identified several bacterial subcommunities within the oral sites that responded similarly to the intervention (**Table 2**). For example, a group of ASVs was significantly more abundant in individuals in the high responder group compared to low responders and represented species of known pathogenic or pro-inflammatory genera such as *Actinomyces*, *Campylobacter*, *Capnocytophaga*, *Fusobacterium*, *Leptotrichia*, and *Porphyromonas* (Huang et al., 2014; Kirst et al., 2015; Kistler et al., 2013; Schincaglia et al., 2017; The Human Microbiome Project Consortium, 2012). Clusters of ASVs that were significantly more abundant in low responders compared to high responders contained known commensal species related to oral

245 health, such as *Kingella oralis* (Abusleme et al., 2021), *Streptococcus* spp. (Caporaso et al., 2011;
246 Zaura et al., 2009), and *Veillonella* spp. (Moore & Moore, 1994). It has to be noted that sequencing
247 based only on the V4 region of the 16S rRNA gene may not provide sufficient resolution to correctly
248 assign pathogenicity or pro-inflammatory traits all ASVs. Similarly, some ASV have been assigned
249 to bacterial taxa that are not commonly observed in the oral cavity; this may indicate that these
250 bacteria were present in the sample due problematic hygiene in the host, or be due to classification
251 errors. Finally, we observed a difference in ecosystem stability between high and low responders in
252 some parts of the oral cavity. This suggests that in some subjects, the ecosystem can withstand the
253 ecological pressure of plaque accumulation and has some mechanisms that prevents healthy
254 microbiota from decreasing in abundance. Further research is needed to identify these mechanisms
255 and the microbiota involved.

256 By integrating the PARAFAC models of the salivary metabolomics data and of the predicted
257 metabolic functions from the microbiome data, we identified enriched pathways that reflected the
258 changing proportions of Gram-positive and -negative microbiota (cell membrane/wall component
259 pathways, such as lipopolysaccharide and peptidoglycan biosynthesis). Quorum sensing systems
260 were found to be significantly enriched in all plaque sites likely due to the presence of various
261 *Streptococcus* spp., that carry genes for oligopeptide binding protein quorum sensing system
262 (Fontaine et al., 2010; Gardan et al., 2009). These are known to regulate biofilm formation and
263 virulence (Hammer & Bassler, 2003; Kong et al., 2006; Preda & Săndulescu, 2019). The strong signal
264 in carbon metabolism and oxidative phosphorylation were likely reflective of the variation in
265 anaerobic bacteria, which accumulate during gingivitis (Chen et al., 2019; Diaz et al., 2002; Loesche,
266 1969). An interesting link between salivary metabolites and microbiome functional potential may
267 have been observed in the nucleoside/purine/pyrimidine biosynthesis pathways: while urea was one
268 of the best modelled salivary metabolites and is a potential biomarker for oral health (D'souza et al.,
269 2023; Gaál Kovalčíková et al., 2019; Nascimento et al., 2009; Osmani, 2023), a role of salivary
270 nucleosides in plaque formation or gingivitis is as yet unknown. While many of these functions can
271 be identified as housekeeping activities, we protected ourselves from wrongfully identifying such
272 generic activities as enriched by (1) using SetRank to correct for multiple pathway membership and
273 (2) creating a custom database of pathway elements and removing very large pathways that often
274 connect to such activities. Further research is needed to investigate the relevance of these enriched
275 pathways in the context of dental plaque formation and gingivitis.

276 In conclusion, we show that PARAFAC modelling of longitudinal oral microbiome and salivary
277 metabolomics data can be used to identify clinically relevant variation and similarly responding
278 microbial subcommunities related to gingivitis. By performing high level integration of predicted
279 microbiome functions and the salivary metabolome, we highlight biochemical pathways of oral
280 biofilm formation and maturation with a likely role in gingivitis.

281 Methods

282 *Data description*

283 The gingivitis challenge study was carried out at the Academic Centre for Dentistry Amsterdam
284 (ACTA) with 15 systemically healthy males and 26 systemically healthy females between the ages
285 of 18 and 55. Recruitment details and exclusion criteria were previously described (Prodan et al.,
286 2016). Reversible gingivitis was induced by omission of oral hygiene during the two-week gingivitis
287 challenge (day 0 to day 14), which was preceded by a two-week baseline period (day -14 to day 0)
288 and followed by a one-week resolution phase (day 14 to day 21; **Figure 1A**). Assessment of plaque
289 formation, bleeding and the collection of oral samples for microbiome were performed throughout
290 the baseline, challenge and resolution phases. Plaque and bleeding were assessed clinically in a half
291 mouth randomized contralateral model (Bentley & Disney, 1995). Oral samples for microbiome
292 analysis were taken at six sites in the mouth: supragingival plaque at the lower and upper jaw lingual
293 surfaces, supragingival plaque at the lower and upper jaw interproximal surfaces, tongue and saliva.
294 The salivary metabolome was only sampled during the challenge phase.

295 *Red fluorescence imaging*

296 Acquisition of red fluorescent plaque (RF) photographs has been described previously (Heinrich-
297 Weltzien et al., 2003; van der Veen et al., 2016; Volgenant et al., 2017). Briefly, fluorescence
298 photographs were taken of the vestibular aspect of the anterior teeth (cuspid to cuspid, upper and
299 lower jaw) in end-to-end position at every time point using a QLF-D camera (Inspektor Research
300 Systems BV, Amsterdam, the Netherlands). The photographs were assessed planimetrically for the
301 percentage red fluorescent protein (RFP) coverage using RFP analysis software (QA2 V1.25,
302 Inspektor Research Systems BV, Amsterdam, the Netherlands). Three response groups were
303 determined using the RF% values on day 14: low (0-1.7%), mid (1.8-6.0%) and high (6.0%+) (**Figure**
304 **1B**) (van der Veen et al., 2016).

305 *DNA isolation and 16S rRNA gene amplicon sequencing*

306 DNA was isolated from the samples using a previously described method (Zaura et al., 2017).
307 Samples were mixed with 300 µl lysis buffer (Agowa, Berlin, Germany), 500 µl phenol saturated
308 with tris-HCl (pH 8.0) and 500 µl zirconium beads (0.1 mm; BioSpec Products, Bartlesville, OK,
309 USA), and shaken in a bead beater for 3 min at 2800 oscillations/min. DNA released was purified
310 using magnetic beads (Agowa, Berlin, Germany) and used for amplicon sequencing.

311 The V4 hypervariable region of the 16S rRNA gene was targeted using primers F515 (5'- GTG CCA
312 GCM GCC GCG GTA A -3') and R806 (5'- GGA CTA CHV GGG TWT CTA AT -3'). The primers
313 included Illumina adapters and a unique 8-nucleotide sample index sequence key (Kozich et al.,
314 2013). PCR was performed using the Phusion Hot Start II High Fidelity PCR Master Mix (Thermo
315 Scientific, Waltham, MA, USA) with 100 pg template. The following amplification program was
316 used: initial denaturation at 98°C for 30 s; 30 cycles of 98°C for 10 s, 55°C for 30 s and 72°C for 30 s;
317 and final elongation at 72°C for 5 min. The amplicon libraries were pooled in equimolar amounts
318 and purified using the QIAquick Gel Extraction Kit (Qiagen, Valencia, CA, USA). Amplicon quality
319 and size were analysed on a Fragment Analyzer (Advanced Analytical Technologies Inc., Ankeny,
320 IA, USA). Amplicon sequencing was performed on the Illumina MiSeq platform (Illumina
321 Technologies, San Diego, CA, USA) using 2 x 200 cycle paired-end settings.

322 *16S rRNA gene amplicon data pre-processing*

323 The 16S rRNA gene sequencing data were pre-processed using DADA2 (version 1.14.0; (Callahan et
324 al., 2016)). All microbiome sampling locations except for saliva were pre-processed with default
325 DADA2 settings (truncLen = c(100, 100), maxN = 0, maxEE = c(2,2), truncQ = 2, rm.phix = TRUE,
326 compress = FALSE, matchIDs = TRUE, multithread = TRUE). The saliva samples were processed
327 with a shorter trimming setting (truncLen = c(200, 215)) due to lower quality reads. Taxonomic
328 classification of ASVs was performed using the SILVA NR99 (v138) and HOMD (v15.22) reference
329 databases.

330 *Metabolomics sampling and profiling*

331 Saliva sample collection and metabolite profiling were described previously (Prodan et al., 2016).
332 Unstimulated saliva was collected at the intervention time points. Participants were instructed to
333 allow saliva to accumulate on the floor of the mouth and to spit at 30 second intervals into a pre-
334 weighted 30 ml polypropylene tube. The collection period was 5 minutes. Non-targeted metabolite
335 profiling of the saliva samples for the gingivitis challenge time points was performed by Metabolon.

336 Samples were processed as described in Metabolon's standard method (Evans et al., 2009). Raw data
337 were extracted, peak-identified and quality controlled using Metabolon's hardware and software.
338 Compounds were identified by comparison with Metabolon's reference library (Lawton et al., 2008).
339 Metabolites were annotated with KEGG compound IDs (Kanehisa et al., 2021; Kanehisa & Goto,
340 2000).

341 *Assessment of clinical parameters of gingivitis*

342 Plaque and bleeding scores were clinically assessed by two experts in a half mouth randomized
343 contralateral model, as described previously (van der Veen et al., 2016). Plaque was quantified using
344 a modified Silness & Loë Plaque Index at six sites of the buccal and lingual aspects of all present
345 teeth (Silness & Löe, 1964). Gingival bleeding was quantified using the bleeding on marginal probing
346 index on six gingival areas on the buccal and lingual sides of all present teeth (Van der Weijden et
347 al., 1993).

348 *Statistical Analysis - Microbiome data processing*

349 The ASV data and taxonomic information were processed using MATLAB (version 2022a). The data
350 were separated by oral site. To limit the sparsity per dataset, ASVs were kept if the sparsity was
351 <50% in any response group (**Supplementary Figure A6**). All other ASVs were removed from the
352 data. By setting a response group-based sparsity-cutoff per ASV, we avoid removing biologically
353 relevant ASVs that would occur in only one or two response groups. ASVs were also removed if
354 they corresponded to chloroplast or mitochondrial sequences, as these were not relevant for the
355 study. An overview of the number of ASVs before and after filtering per sample type is reported in
356 **Supplementary Table B5**. Subsequently, a centered-log ratio transformation - using a pseudo-count
357 of 1 - was performed to correct for compositionality (Aitchison, 1982; Gloor et al., 2017). The
358 datasets were then converted to three-way arrays (**Figure 1D**). Missing samples were kept in the
359 data cube as a row of missing values (**Supplementary Table B6**). This is possible because PARAFAC
360 interpolates the missing data automatically in its alternating least-squares algorithm and maximises
361 the amount of information for the modelling procedure as the other samples of the subject do not
362 have to be removed entirely. Subsequently, centering across the subject mode and scaling within
363 the ASV mode - ignoring missing values - was performed to make the samples comparable at every
364 timepoint and the ASVs comparable for all time points (Bro & Smilde, 2003).

365 *Statistical Analysis - Salivary metabolomics data processing*

366 The salivary metabolomics data were processed using MATLAB (version 2022a). To limit the
367 sparsity per dataset, metabolites were excluded if they contained more than 25% values below the
368 detection limit (**Supplementary Figure A7**). Additionally, xenobiotic compounds were manually
369 assessed for occurrence across response groups and selected if they were prevalent in most subjects
370 (**Supplementary Data**). After feature selection, 400 of the 499 metabolites remained (**Supplementary**
371 **Table B5**). Values below the detection limit were imputed with a random value between 0 and the
372 detection limit per metabolite to preserve their distribution. To correct for the dilution caused by
373 the amount of water in the saliva samples, Probabilistic Quotient Normalization (PQN) was
374 performed using the median value of each metabolite as an artificial reference sample (Dieterle et
375 al., 2006). Next, the dataset was (natural) log transformed to stabilize the variance. The dataset was
376 then converted to a three-way array. Subsequently, centering across the subject mode and scaling
377 within the ASV mode - ignoring missing values - was performed to make the samples comparable
378 at every timepoint and the ASVs comparable for all time points (Bro & Smilde, 2003). All subjects
379 were fully sampled, except for subject 3CN8CB for whom no metabolome data was available
380 (**Supplementary Table B6**).

381 *Functional profile prediction of microbiome data*

382 A functional profile prediction based on the microbiome ASV count data was performed using the
383 Tax4Fun2 package in R (Tax4Fun2 version 1.1.5, R version 4.0.3) (Aßhauer et al., 2015; Wemheuer
384 et al., 2020). ASVs corresponding to Chloroplast or Mitochondria were removed. Samples were
385 rarefied to 10 000 reads to make them comparable (**Supplementary Figures A8** and **A9**). Samples with
386 fewer total reads were removed. This step removed 53 of 1 692 samples. ASVs without counts after
387 rarefying were removed. All steps together removed 6 903 out of 14 014 ASVs. Tax4Fun2 was run
388 with default settings against the included Ref99NR database (Wemheuer et al., 2020) and a custom
389 database based on the HOMD genomes (v9.14, accessed 2020-11-09) (Chen et al., 2010). Molecular
390 functions of the genomes were assigned using Tax4Fun2's DIAMOND wrapper (Buchfink et al.,
391 2015). HOMD-annotated 16S rRNA gene sequences were extracted from the genomes, cut to the
392 515F-806R fragment used in this study using cutadapt v1.18 (Martin, 2011). Exact duplication
393 within genomes were removed, and 16S rRNA gene sequence fragments were combined with the
394 functional assignments using Tax4Fun's generateUserDataByClustering function. The resulting
395 functional prediction profiles - which contain values between 0 and 1 for each function - were used

396 for subsequent analysis. The fraction of unused taxonomic units and the fraction of unused
397 sequences are reported per sample (**Supplementary Figures A10** and **A11**).

398 *Statistical Analysis - Processing of functional profile predictions*

399 The functionally predicted microbiome data were processed in MATLAB (version 2022a). The data
400 were separated by sample type. To make the data comparable to the salivary metabolomics data,
401 predicted KEGG orthologous groups (KOs) were removed if they did not belong to pathways that
402 the metabolites mapped to. This was done by mapping the KOs and metabolite compound IDs to
403 pathways using the KEGG API (Kawashima et al., 2003). To limit the sparsity per dataset, KOs were
404 removed if the number of zeroes for all response groups was >50% (**Supplementary Figure A12**).
405 Additionally, KOs were removed if the sum-of-squares was lower than 0.025% of the total sum-of-
406 squares of the dataset (**Supplementary Figure A13**). This latter filter was to ensure that the modelling
407 procedure focused on relevant variation in the data and made the total number of variables
408 comparable to the metabolomics data, while retaining most information. An overview of the
409 number of KOs remaining after feature selection is reported (**Supplementary Table B5**).
410 Subsequently a centered-log ratio transformation of each dataset was performed to correct for
411 compositionality (Aitchison, 1982; Gloor et al., 2017). The dataset was then converted to a three-
412 way array. Missing samples were kept in the data cube as a row of missing values (**Supplementary**
413 **Table B6**). Subsequently, centering across the subject mode and scaling within the ASV mode -
414 ignoring missing values - was performed to make the samples comparable at every timepoint and
415 the ASVs comparable for all time points (Bro & Smilde, 2003).

416 *Statistical Analysis - Parallel Factor Analysis (PARAFAC)*

417 Details on the creation of PARAFAC models for microbiome (Martino et al., 2021) and
418 metabolomics data (Bro, 1997) have been described elsewhere. The PARAFAC implementation
419 from the N-way toolbox (version 1.8.0.0) in MATLAB (version 2022a) was used to create PARAFAC
420 models for all datasets (Bro, accessed 26-10-2023). Similar to PCA, the correct number of
421 components of the PARAFAC model needed to be determined to create an optimal model (Bro &
422 Kiers, 2003; van der Ploeg et al., 2024). This was done by inspecting the number of iterations needed
423 to converge (Bro, 1997), the core consistency diagnostic (CORCONDIA) (Bro & Kiers, 2003), the
424 variation explained (Bro, 1997), and the Tucker congruence coefficient per mode (Lorenzo-Seva &
425 ten Berge, 2006; Tucker, 1951). Additionally, a jack-knife approach was used to determine the

426 stability of the PARAFAC modelling procedure. These metrics were inspected per component for
427 every generated model (**Supplementary Data**). All generated models are reported in **Supplementary**
428 **Figures A14-A26**. An overview of the model statistics also reported (**Supplementary Table B7**).
429 Congruence loadings, which describe the relationships between the original variables of the dataset
430 and the latent variables of the corresponding model, were calculated for every component in every
431 sample type (Lorho et al., 2006). While the metrics above suggested a one-component PARAFAC
432 model corresponding to the microbiome data at the lower jaw interproximal niche, the model
433 described less than 10% of the variation in the data. Furthermore, manual inspection revealed that
434 the model did not describe variation that we could explain biologically. Hence, we did not analyse
435 this model further in subsequent steps.

436 A transformation of the subject loadings was required for comparison with the longitudinally
437 measured clinical parameters of gingivitis. The ASV loading vectors were orthonormalized using
438 the Gram-Schmidt orthonormalization procedure in the pracma R package (version 2.4.2) (Borchers
439 & Borchers, 2022; Schmidt, 1989). The (same) transformation matrix is then applied to the
440 Kronecker product of the subject and the time loadings to obtain interpretable loadings of every
441 subject-time combination (Kiers, 2000). The correlation of the time-resolved subject loadings with
442 the clinical parameters of gingivitis was then tested (**Table 1** and **Supplementary Table B1**).

443 *Statistical Analysis - Microbiome ASV cluster analysis*

444 Loading plots of the ASV mode and the subject mode for each of the microbiome PARAFAC models
445 were created (**Figure 2**). ASVs were filtered out if they had a variation explained lower than the
446 average of the model or a congruence loading lower than 0.4 (Lorho et al., 2006). ASVs were
447 clustered based on their fitted abundances according to the PARAFAC model using the K-medoids
448 algorithm from the cluster R package (version 2.1.4) with 50 random starts to be robust against
449 outliers (Maechler, 2019). The number of clusters was determined using the within-cluster sum of
450 squares, silhouette width and gap statistic metrics as reported by the factoextra R package (version
451 1.0.7, **Supplementary Figure A27**) (Kassambara & Mundt, 2017). An overview of the taxonomic
452 information per cluster can be found in **Table 2**. Bacteria in **Table 2** were only reported if two criteria
453 were met: (1) the taxonomic classification was resolved to species level by DADA2 using the SILVA
454 (v138) and HOMD (v15.22) databases and (2) the annotation agreed with a separate best hit
455 annotation run using the HOMD (v15.22) database. Cases where the classification was resolved to

species level by the DADA2 run but only to the genus level by the separate HOMD run are also reported.

The response to the gingivitis intervention of the ASV clusters was shown using the relative abundance sum per ASV cluster derived from the original count data (**Figure 3** and **Supplementary Figure A3**). The mean of the summed relative abundances and standard error of the mean were calculated per response group for a given sample type and time point. The mean difference between the high and low responders was tested using a permutation analysis where the response group membership of the subjects was permuted (**Supplementary Table B2**).

Statistical Analysis - Functional enrichment analysis

The PARAFAC models of the functionally profiled microbiome and salivary metabolomics data were combined to perform a pathway enrichment test per sample type. This was done by calculating the variance explained and congruence loadings per KO or metabolite in each model (Lorho et al., 2006). If the PARAFAC model contained two components, the maximum of the two congruence loadings per feature was used. The variance explained and congruences were normalized by the maximum value per model prior to integration. The normalized variance explained and normalized congruence per feature were averaged to obtain a ranking of pathway elements (KOs and metabolites). This causes the best modelled KO and compound ID to be at the top of this list. The ranked pathway element list was cut off at 75% of its length to ensure a good separation between well-modelled and averagely-modelled pathway elements (**Supplementary Figure A28**).

The SetRank R package (version 1.1.0) was used to obtain pathways of interest (Simillion et al., 2017). SetRank is a gene set enrichment algorithm that obtains a high sensitivity by correcting for multiple pathway membership. A custom database of pathway elements was created by combining the KO and compound ID to pathway mappings obtained through the KEGG API (**Supplementary Data**). Pathways were removed from our database if they could not be performed by prokaryotes. Generic, large pathways with more than 750 elements were removed to ensure that the enrichment results were specific enough for interpretation (**Supplementary Figure A29**). Subsequently the SetRank analysis was performed with standard settings per sample type. The multiple-pathway corrected p-values are reported ($p \leq 0.05$, **Figure 4** and **Supplementary Table B4**)

Data Availability

The ASV abundance data is available at https://github.com/GRvanderPloeg/TIFN-multiway. Raw sequencing data is available by request from the authors, in accordance with the informed consent signed by the study participants.

Code Availability

The underlying code for this study is available on GitHub and can be accessed via https://github.com/GRvanderPloeg/TIFN-multiway/releases/tag/v1.2.

Ethics statement

The study involving human participants was conducted in accordance with the ethical principles of the 64th WMA Declaration of Helsinki (October 2013, Brazil) and the Medical Research Involving Human Subjects Act (WMO), approximating Good clinical Practice (CPMP/ICH/135/95) guidelines. The clinical trial was approved by the Medical Ethical Committee of the VU Medical Center (2014.505) and registered at the public trial register of the Central Committee on Research Involving Human Subjects (CCMO) under number NL51111.029.14.

Author Contributions

G.R. van der Ploeg: formal analysis, methodology, writing - original draft; B.W. Brandt: investigation, writing - review & editing; B.J.F. Keijser: investigation, project administration, writing - review & editing; M.H. van der Veen: investigation, project administration, writing - review & editing; C.M.C. Volgenant: investigation, writing - review & editing; E. Zaura: conceptualization, investigation, project administration, funding acquisition, writing - review & editing; A.K. Smilde: conceptualization, methodology, supervision, funding acquisition, writing - review & editing; J.A. Westerhuis: conceptualization, methodology, supervision, formal analysis, writing - original draft; A. Heintz-Buschart: conceptualization, formal analysis, supervision, project administration, writing - original draft. All authors reviewed and approved the manuscript.

Competing interests

The authors declare that the research was conducted in the absence of any commercial or financial relationships that could be construed as a potential conflict of interest.

Acknowledgements

We want to thank Michelle van der Wurff (TNO) and Tim van den Broek (TNO) for their help in data acquisition, processing and storing and Jesse Alderliesten (UU/UvA), Fred White (UvA), Cynthia

Albracht (UvA), Juan Pablo Bascur (CWTS) and Rianne Warmerdam (Aiden) for their useful discussions and suggestions. The authors thank N.A.M. Rosema for coordinating the clinical study. For assistance in capturing fluorescence photographs, the authors thank Y. Altindağ. For the clinical examinations the authors thank J.M. Voll (clinical plaque assessment with Silness & Löe), and S. Bizzarro (assessment of the bleeding on marginal probing).

This research is supported by the Dutch Technology Foundation STW (project number 10948) and the Top Institute Food and Nutrition (TIFN), a public-private partnership on precompetitive research in food and nutrition. Organizations supporting this project had no role in study design, data collection and analysis, decision to publish, or preparation of the manuscript. QLF data was obtained with funding from NWO (ZonMw-STW-NIG-program): "Project 10948: Seeing is believing? A novel tool for the visualization of oral disease manifestations." GRvdP was funded by a grant from the University of Amsterdam, Research Priority Area on Personal Microbiome Health.

References

Abusleme, L., Hoare, A., Hong, B., & Diaz, P. I. (2021). Microbial signatures of health, gingivitis, and periodontitis. *Periodontology 2000*, *86*(1), 57–78. https://doi.org/10.1111/prd.12362

Acar, E., Bro, R., & Smilde, A. (2015). Data Fusion in Metabolomics Using Coupled Matrix and Tensor Factorizations. *Proceedings of the IEEE*, *103*, 1602. https://doi.org/10.1109/JPROC.2015.2438719

Acar, E., Papalexakis, E. E., Gürdeniz, G., Rasmussen, M. A., Lawaetz, A. J., Nilsson, M., & Bro, R. (2014). Structure-revealing data fusion. *BMC Bioinformatics*, *15*(1), 239. https://doi.org/10.1186/1471-2105-15-239

Aitchison, J. (1982). The Statistical Analysis of Compositional Data. *Journal of the Royal Statistical Society: Series B (Methodological)*, *44*(2), 139–160. https://doi.org/10.1111/j.2517-6161.1982.tb01195.x

Anderson, A. C., Rothballer, M., Altenburger, M. J., Woelber, J. P., Karygianni, L., Lagkouvardos, I., Hellwig, E., & Al-Ahmad, A. (2018). In-vivo shift of the microbiota in oral biofilm in response to

541 frequent sucrose consumption. *Scientific Reports*, *8*(1), Article 1.
542 https://doi.org/10.1038/s41598-018-32544-6
543 Aßhauer, K. P., Wemheuer, B., Daniel, R., & Meinicke, P. (2015). Tax4Fun: Predicting functional profiles
544 from metagenomic 16S rRNA data. *Bioinformatics*, *31*(17), 2882–2884.
545 https://doi.org/10.1093/bioinformatics/btv287
546 Axelsson, P., Lindhe, J., & Nyström, B. (1991). On the prevention of caries and periodontal disease.
547 *Journal of Clinical Periodontology*, *18*(3), 182–189. https://doi.org/10.1111/j.1600-
548 051X.1991.tb01131.x
549 Baker, J. L., Bor, B., Agnello, M., Shi, W., & He, X. (2017). Ecology of the Oral Microbiome: Beyond
550 Bacteria. *Trends in Microbiology*, *25*(5), 362–374. https://doi.org/10.1016/j.tim.2016.12.012
551 Bentley, C. D., & Disney, J. A. (1995). A comparison of partial and full mouth scoring of plaque and
552 gingivitis in oral hygiene studies. *Journal of Clinical Periodontology*, *22*(2), 131–135.
553 https://doi.org/10.1111/j.1600-051X.1995.tb00124.x
554 Bergström, J., & Preber, H. (1986). The influence of cigarette smoking on the development of
555 experimental gingivitis. *Journal of Periodontal Research*, *21*(6), 668–676.
556 https://doi.org/10.1111/j.1600-0765.1986.tb01504.x
557 Borchers, H. W., & Borchers, M. H. W. (2022). Package 'pracma.' *Accessed On*, *4*.
558 https://mirror.las.iastate.edu/CRAN/web/packages/pracma/pracma.pdf
559 Bro, R. (n.d.). *The N-way Toolbox*. Retrieved October 26, 2023, from
560 https://nl.mathworks.com/matlabcentral/fileexchange/1088-the-n-way-toolbox
561 Bro, R. (1996). Multiway calibration. Multilinear PLS. *Journal of Chemometrics*, *10*(1), 47–61.
562 https://doi.org/10.1002/(SICI)1099-128X(199601)10:1<47::AID-CEM400>3.0.CO;2-C
563 Bro, R. (1997). PARAFAC. Tutorial and applications. *Chemometrics and Intelligent Laboratory Systems*.
564 Bro, R., & Kiers, H. (2003). A new Efficient Method for Determining the Number of Components in
565 PARAFAC Models. *Journal of Chemometrics*, *17*, 274–286. https://doi.org/10.1002/cem.801

566 Bro, R., & Smilde, A. K. (2003). Centering and scaling in component analysis. *Journal of Chemometrics*,
567 *17*(1), 16–33. https://doi.org/10.1002/cem.773
568 Buchfink, B., Xie, C., & Huson, D. H. (2015). Fast and sensitive protein alignment using DIAMOND.
569 *Nature Methods*, *12*(1), 59–60.
570 Callahan, B. J., McMurdie, P. J., Rosen, M. J., Han, A. W., Johnson, A. J. A., & Holmes, S. P. (2016).
571 DADA2: High-resolution sample inference from Illumina amplicon data. *Nature Methods*,
572 *13*(7), Article 7. https://doi.org/10.1038/nmeth.3869
573 Caporaso, J. G., Lauber, C. L., Costello, E. K., Berg-Lyons, D., Gonzalez, A., Stombaugh, J., Knights, D.,
574 Gajer, P., Ravel, J., Fierer, N., Gordon, J. I., & Knight, R. (2011). Moving pictures of the human
575 microbiome. *Genome Biology*, *12*(5), R50. https://doi.org/10.1186/gb-2011-12-5-r50
576 Carroll, J. D., & Chang, J.-J. (1970). Analysis of individual differences in multidimensional scaling via an
577 n-way generalization of "Eckart-Young" decomposition. *Psychometrika*, *35*(3), 283–319.
578 https://doi.org/10.1007/BF02310791
579 Chapple, I. L. C., Mealey, B. L., Van Dyke, T. E., Bartold, P. M., Dommisch, H., Eickholz, P., Geisinger, M.
580 L., Genco, R. J., Glogauer, M., Goldstein, M., Griffin, T. J., Holmstrup, P., Johnson, G. K., Kapila,
581 Y., Lang, N. P., Meyle, J., Murakami, S., Plemons, J., Romito, G. A., … Yoshie, H. (2018).
582 Periodontal health and gingival diseases and conditions on an intact and a reduced
583 periodontium: Consensus report of workgroup 1 of the 2017 World Workshop on the
584 Classification of Periodontal and Peri-Implant Diseases and Conditions. *Journal of*
585 *Periodontology*, *89*, S74–S84. https://doi.org/10.1002/JPER.17-0719
586 Chapple, I. L. C., Van der Weijden, F., Doerfer, C., Herrera, D., Shapira, L., Polak, D., Madianos, P.,
587 Louropoulou, A., Machtei, E., Donos, N., Greenwell, H., Van Winkelhoff, A. J., Eren Kuru, B.,
588 Arweiler, N., Teughels, W., Aimetti, M., Molina, A., Montero, E., & Graziani, F. (2015). Primary
589 prevention of periodontitis: Managing gingivitis. *Journal of Clinical Periodontology*, *42*(S16),
590 S71–S76. https://doi.org/10.1111/jcpe.12366

591 Chen, M., Cai, W., Zhao, S., Shi, L., Chen, Y., Li, X., Sun, X., Mao, Y., He, B., Hou, Y., Zhou, Y., Zhou, Q.,
592 Ma, J., & Huang, S. (2019). Oxidative stress-related biomarkers in saliva and gingival crevicular
593 fluid associated with chronic periodontitis: A systematic review and meta-analysis. *Journal of*
594 *Clinical Periodontology*, *46*(6), 608–622. https://doi.org/10.1111/jcpe.13112
595 Chen, T., Yu, W.-H., Izard, J., Baranova, O. V., Lakshmanan, A., & Dewhirst, F. E. (2010). The Human Oral
596 Microbiome Database: A web accessible resource for investigating oral microbe taxonomic and
597 genomic information. *Database*, *2010*.
598 https://academic.oup.com/database/article/doi/10.1093/database/baq013/405450?view=lo
599 ng
600 Curtis, M. A., Diaz, P. I., & Van Dyke, T. E. (2020). The role of the microbiota in periodontal disease.
601 *Periodontology 2000*, *83*(1), 14–25. https://doi.org/10.1111/prd.12296
602 Dawes, C., & Wong, D. T. W. (2019). Role of Saliva and Salivary Diagnostics in the Advancement of Oral
603 Health. *Journal of Dental Research*, *98*(2), 133–141.
604 https://doi.org/10.1177/0022034518816961
605 Diaz, P. I., Hoare, A., & Hong, B.-Y. (2016). Subgingival Microbiome Shifts and Community Dynamics in
606 Periodontal Diseases. *Journal of the California Dental Association*, *44*(7), 421–435.
607 https://doi.org/10.1080/19424396.2016.12221035
608 Diaz, P. I., Zilm, P. S., & Rogers, A. H. (2002). Fusobacterium nucleatum supports the growth of
609 Porphyromonas gingivalis in oxygenated and carbon-dioxide-depleted environments.
610 *Microbiology*, *148*(2), 467–472. https://doi.org/10.1099/00221287-148-2-467
611 Dieterle, F., Ross, A., Schlotterbeck, G., & Senn, H. (2006). Probabilistic Quotient Normalization as
612 Robust Method to Account for Dilution of Complex Biological Mixtures. Application in 1H NMR
613 Metabonomics. *Analytical Chemistry*, *78*(13), 4281–4290. https://doi.org/10.1021/ac051632c
614 D'souza, L. L., Lawande, S. A., Samuel, J., & Pinto, M. J. W. (2023). Effect of salivary urea, pH and
615 ureolytic microflora on dental calculus formation and its correlation with periodontal status.
616 *Journal of Oral Biology and Craniofacial Research*, *13*(1), 8–12.

617 Evans, A. M., DeHaven, C. D., Barrett, T., Mitchell, M., & Milgram, E. (2009). Integrated, Nontargeted
618 Ultrahigh Performance Liquid Chromatography/Electrospray Ionization Tandem Mass
619 Spectrometry Platform for the Identification and Relative Quantification of the Small-Molecule
620 Complement of Biological Systems. *Analytical Chemistry*, *81*(16), 6656–6667.
621 https://doi.org/10.1021/ac901536h
622 Fontaine, L., Boutry, C., De Frahan, M. H., Delplace, B., Fremaux, C., Horvath, P., Boyaval, P., & Hols, P.
623 (2010). A Novel Pheromone Quorum-Sensing System Controls the Development of Natural
624 Competence in *Streptococcus thermophilus* and *Streptococcus salivarius*. *Journal of*
625 *Bacteriology*, *192*(5), 1444–1454. https://doi.org/10.1128/JB.01251-09
626 Gaál Kovalčíková, A., Pančíková, A., Konečná, B., Klamárová, T., Novák, B., Kovaľová, E., Podracká, Ľ.,
627 Celec, P., & Tóthová, Ľ. (2019). Urea and creatinine levels in saliva of patients with and without
628 periodontitis. *European Journal of Oral Sciences*, *127*(5), 417–424.
629 https://doi.org/10.1111/eos.12642
630 Gardan, R., Besset, C., Guillot, A., Gitton, C., & Monnet, V. (2009). The Oligopeptide Transport System
631 Is Essential for the Development of Natural Competence in *Streptococcus thermophilus* Strain
632 LMD-9. *Journal of Bacteriology*, *191*(14), 4647–4655. https://doi.org/10.1128/JB.00257-09
633 Gloor, G. B., Macklaim, J. M., Pawlowsky-Glahn, V., & Egozcue, J. J. (2017). Microbiome Datasets Are
634 Compositional: And This Is Not Optional. *Frontiers in Microbiology*, *8*, 2224.
635 https://doi.org/10.3389/fmicb.2017.02224
636 Guk, H.-J., Lee, E.-S., Jung, U.-W., & Kim, B.-I. (2020). Red fluorescence of Interdental plaque for
637 screening of gingival health. *Photodiagnosis and Photodynamic Therapy*, *29*, 101636.
638 https://doi.org/10.1016/j.pdpdt.2019.101636
639 Hammer, B. K., & Bassler, B. L. (2003). Quorum sensing controls biofilm formation in *Vibrio cholerae*.
640 *Molecular Microbiology*, *50*(1), 101–104. https://doi.org/10.1046/j.1365-2958.2003.03688.x

Han, L., Gao, X., Liao, M., Yu, X., Zhang, R., Liu, S., & Zeng, F. (2020). Hygiene practices among young adolescents aged 12-15 years in low- and middle-income countries: A population-based study. *Journal of Global Health*, *10*(2), 020436. https://doi.org/10.7189/jogh.10.020436

Harshman, R. A. (1970). *Foundations of the PARAFAC procedure: Models and conditions for an" explanatory" multimodal factor analysis*. https://www.psychology.uwo.ca/faculty/harshman/wpppfac0.pdf

Heinrich-Weltzien, R., Kühnisch, J., Van Der Veen, M., De Josselin De Jong, E., & Stößer, L. (2003). Quantitative light-induced fluorescence (QLF)—A potential method for the dental practitioner. *Quintessence International*, *34*(3), 181–188.

Huang, S., Li, R., Zeng, X., He, T., Zhao, H., Chang, A., Bo, C., Chen, J., Yang, F., Knight, R., Liu, J., Davis, C., & Xu, J. (2014). Predictive modeling of gingivitis severity and susceptibility via oral microbiota. *The ISME Journal*, *8*(9), 1768–1780. https://doi.org/10.1038/ismej.2014.32

Kanehisa, M., Furumichi, M., Sato, Y., Ishiguro-Watanabe, M., & Tanabe, M. (2021). KEGG: Integrating viruses and cellular organisms. *Nucleic Acids Research*, *49*(D1), D545–D551. https://doi.org/10.1093/nar/gkaa970

Kanehisa, M., & Goto, S. (2000). KEGG: Kyoto Encyclopedia of Genes and Genomes. *Nucleic Acids Research*, *28*(1), 27–30. https://doi.org/10.1093/nar/28.1.27

Kassambara, A., & Mundt, F. (2017). Package 'factoextra.' *Extract and Visualize the Results of Multivariate Data Analyses*, *76*(2). https://piyanit.nl/wp-content/uploads/2020/10/factoextra.pdf

Kawashima, S., Katayama, T., Sato, Y., & Kanehisa, M. (2003). KEGG API: A Web Service Using SOAP/WSDL to Access the KEGG System. *Genome Informatics*, *14*, 673–674. https://doi.org/10.11234/gi1990.14.673

Kiers, H. A. L. (2000). Some procedures for displaying results from three-way methods. *Journal of Chemometrics*, *14*(3), 151–170. https://doi.org/10.1002/1099-128X(200005/06)14:3<151::AID-CEM585>3.0.CO;2-G

667 Kilian, M., Chapple, I. L. C., Hannig, M., Marsh, P. D., Meuric, V., Pedersen, A. M. L., Tonetti, M. S.,
668 Wade, W. G., & Zaura, E. (2016). The oral microbiome – an update for oral healthcare
669 professionals. *British Dental Journal*, *221*(10), Article 10.
670 https://doi.org/10.1038/sj.bdj.2016.865
671 Kirst, M. E., Li, E. C., Alfant, B., Chi, Y.-Y., Walker, C., Magnusson, I., & Wang, G. P. (2015). Dysbiosis and
672 Alterations in Predicted Functions of the Subgingival Microbiome in Chronic Periodontitis.
673 *Applied and Environmental Microbiology*, *81*(2), 783–793.
674 https://doi.org/10.1128/AEM.02712-14
675 Kistler, J. O., Booth, V., Bradshaw, D. J., & Wade, W. G. (2013). Bacterial Community Development in
676 Experimental Gingivitis. *PLoS ONE*, *8*(8), e71227.
677 https://doi.org/10.1371/journal.pone.0071227
678 Kong, K.-F., Vuong, C., & Otto, M. (2006). Staphylococcus quorum sensing in biofilm formation and
679 infection. *International Journal of Medical Microbiology*, *296*(2–3), 133–139.
680 König, K. G., & Navia, J. M. (1995). Nutritional role of sugars in oral health. *The American Journal of*
681 *Clinical Nutrition*, *62*(1), 275S-282S.
682 Kozich, J. J., Westcott, S. L., Baxter, N. T., Highlander, S. K., & Schloss, P. D. (2013). Development of a
683 Dual-Index Sequencing Strategy and Curation Pipeline for Analyzing Amplicon Sequence Data
684 on the MiSeq Illumina Sequencing Platform. *Applied and Environmental Microbiology*, *79*(17),
685 5112–5120. https://doi.org/10.1128/AEM.01043-13
686 Lawton, K. A., Berger, A., Mitchell, M., Milgram, K. E., Evans, A. M., Guo, L., Hanson, R. W., Kalhan, S.
687 C., Ryals, J. A., & Milburn, M. V. (2008). Analysis of the adult human plasma metabolome.
688 *Pharmacogenomics*, *9*(4), 383–397. https://doi.org/10.2217/14622416.9.4.383
689 Löe, H., Theilade, E., & Jensen, S. B. (1965). Experimental Gingivitis in Man. *Journal of Periodontology*,
690 *36*(3), 177–187. https://doi.org/10.1902/jop.1965.36.3.177
691 Loesche, W. J. (1969). Oxygen Sensitivity of Various Anaerobic Bacteria. *Applied Microbiology*, *18*(5),
692 723–727. https://doi.org/10.1128/am.18.5.723-727.1969

Lorenzo-Seva, U., & ten Berge, J. M. F. (2006). Tucker's congruence coefficient as a meaningful index of factor similarity. *Methodology: European Journal of Research Methods for the Behavioral and Social Sciences*, *2*(2), 57–64. https://doi.org/10.1027/1614-2241.2.2.57

Lorho, G., Westad, F., & Bro, R. (2006). Generalized correlation loadings: Extending correlation loadings to congruence and to multi-way models. *Chemometrics and Intelligent Laboratory Systems*, *84*(1), 119–125. https://doi.org/10.1016/j.chemolab.2006.04.023

Maechler, M. (2019). Finding groups in data: Cluster analysis extended Rousseeuw et al. *R Package Version*, *2*(0), 242–248.

Marsh, P. D. (1991). Sugar, fluoride, pH and microbial homeostasis in dental plaque. *Proceedings of the Finnish Dental Society. Suomen Hammaslaakariseuran Toimituksia*, *87*(4), 515–525.

Martin, M. (2011). Cutadapt removes adapter sequences from high-throughput sequencing reads. *EMBnet. Journal*, *17*(1), 10–12.

Martino, C., Shenhav, L., Marotz, C. A., Armstrong, G., McDonald, D., Vázquez-Baeza, Y., Morton, J. T., Jiang, L., Dominguez-Bello, M. G., Swafford, A. D., Halperin, E., & Knight, R. (2021). Context-aware dimensionality reduction deconvolutes gut microbial community dynamics. *Nature Biotechnology*, *39*(2), 165–168. https://doi.org/10.1038/s41587-020-0660-7

Moore, W. E. C., & Moore, L. V. H. (1994). The bacteria of periodontal diseases. *Periodontology 2000*, *5*(1), 66–77. https://doi.org/10.1111/j.1600-0757.1994.tb00019.x

Murakami, S., Mealey, B. L., Mariotti, A., & Chapple, I. L. C. (2018). Dental plaque–induced gingival conditions. *Journal of Clinical Periodontology*, *45*(S20), S17–S27. https://doi.org/10.1111/jcpe.12937

Nascimento, M. M., Gordan, V. V., Garvan, C. W., Browngardt, C. M., & Burne, R. A. (2009). Correlations of oral bacterial arginine and urea catabolism with caries experience. *Oral Microbiology and Immunology*, *24*(2), 89–95. https://doi.org/10.1111/j.1399-302X.2008.00477.x

717 Nibali, L., Di Iorio, A., Tu, Y., & Vieira, A. R. (2017). Host genetics role in the pathogenesis of periodontal
718 disease and caries. *Journal of Clinical Periodontology*, *44*(S18).
719 https://doi.org/10.1111/jcpe.12639
720 Nobbs, A. H., & Jenkinson, H. F. (2015). Interkingdom networking within the oral microbiome. *Microbes*
721 *and Infection*, *17*(7), 484–492. https://doi.org/10.1016/j.micinf.2015.03.008
722 Odom, A. R. (2011). Five questions about non-mevalonate isoprenoid biosynthesis. *PLoS Pathogens*,
723 *7*(12), e1002323.
724 Osmani, F. (2023). Can the salivary urea and stimulated saliva concentration be a marker of periodontal
725 diseases in opioid users? A case-control study. *Heliyon*, *9*(7).
726 https://www.cell.com/heliyon/pdf/S2405-8440(23)04301-3.pdf
727 Peres, M. A., Macpherson, L. M. D., Weyant, R. J., Daly, B., Venturelli, R., Mathur, M. R., Listl, S., Celeste,
728 R. K., Guarnizo-Herreño, C. C., Kearns, C., Benzian, H., Allison, P., & Watt, R. G. (2019). Oral
729 diseases: A global public health challenge. *The Lancet*, *394*(10194), 249–260.
730 https://doi.org/10.1016/S0140-6736(19)31146-8
731 Petersen, P. E., Bourgeois, D., Ogawa, H., Estupinan-Day, S., & Ndiaye, C. (2005). The global burden of
732 oral diseases and risks to oral health. *Bulletin of the World Health Organization*.
733 Preda, V. G., & Săndulescu, O. (2019). Communication is the key: Biofilms, quorum sensing, formation
734 and prevention. *Discoveries*, *7*(3). https://www.ncbi.nlm.nih.gov/pmc/articles/PMC7086079/
735 Proctor, G. B. (2016). The physiology of salivary secretion. *Periodontology 2000*, *70*(1), 11–25.
736 https://doi.org/10.1111/prd.12116
737 Prodan, A., Imangaliyev, S., Brand, H. S., Rosema, M. N. A., Levin, E., Crielaard, W., Keijser, B. J. F., &
738 Veerman, E. C. I. (2016). Effect of experimental gingivitis induction and erythritol on the
739 salivary metabolome and functional biochemistry of systemically healthy young adults.
740 *Metabolomics*, *12*(9), 147. https://doi.org/10.1007/s11306-016-1096-4
741 Schincaglia, G. P., Hong, B. Y., Rosania, A., Barasz, J., Thompson, A., Sobue, T., Panagakos, F., Burleson,
742 J. A., Dongari-Bagtzoglou, A., & Diaz, P. I. (2017). Clinical, Immune, and Microbiome Traits of

Gingivitis and Peri-implant Mucositis. *Journal of Dental Research*, *96*(1), 47–55. https://doi.org/10.1177/0022034516668847

Schmidt, E. (1989). Über die Auflösung Linearer Gleichungen mit Unendlich Vielen Unbekannten. In A. Pietsch (Ed.), *Integralgleichungen und Gleichungen mit unendlich vielen Unbekannten* (Vol. 11, pp. 249–278). Springer Vienna. https://doi.org/10.1007/978-3-7091-9535-2_5

Schoilew, K., Ueffing, H., Dalpke, A., Wolff, B., Frese, C., Wolff, D., & Boutin, S. (2019). Bacterial biofilm composition in healthy subjects with and without caries experience. *Journal of Oral Microbiology*, *11*(1), 1633194. https://doi.org/10.1080/20002297.2019.1633194

Silness, J., & Löe, H. (1964). Periodontal Disease in Pregnancy II. Correlation Between Oral Hygiene and Periodontal Condition. *Acta Odontologica Scandinavica*, *22*(1), 121–135. https://doi.org/10.3109/00016356408993968

Simillion, C., Liechti, R., Lischer, H. E. L., Ioannidis, V., & Bruggmann, R. (2017). Avoiding the pitfalls of gene set enrichment analysis with SetRank. *BMC Bioinformatics*, *18*(1), 151. https://doi.org/10.1186/s12859-017-1571-6

Singh, A. P., & Gordon, G. J. (2008). Relational learning via collective matrix factorization. *Proceedings of the 14th ACM SIGKDD International Conference on Knowledge Discovery and Data Mining*, 650–658. https://doi.org/10.1145/1401890.1401969

Ter Steeg, P. F., Van Der Hoeven, J. S., De Jong, M. H., Van Munster, P. J. J., & Jansen, M. J. H. (1988). Modelling the Gingival Pocket by Enrichment of Subgingival Microflora in Human Serum in Chemostats. *Microbial Ecology in Health and Disease*, *1*(2), 73–84. https://doi.org/10.3109/08910608809140185

The Human Microbiome Project Consortium. (2012). Structure, function and diversity of the healthy human microbiome. *Nature*, *486*(7402), 207–214. https://doi.org/10.1038/nature11234

Thomas, A. M., Gleber-Netto, F. O., Fernandes, G. R., Amorim, M., Barbosa, L. F., Francisco, A. L. N., Guerra de Andrade, A., Setubal, J. C., Kowalski, L. P., Nunes, D. N., & Dias-Neto, E. (2014).

Alcohol and tobacco consumption affects bacterial richness in oral cavity mucosa biofilms. *BMC Microbiology*, *14*(1), 250. https://doi.org/10.1186/s12866-014-0250-2

Tucker, L. R. (1951). *A method for synthesis of factor analysis studies* (Vol. 984). Educational Testing Service Princeton, NJ. https://apps.dtic.mil/sti/pdfs/AD0047524.pdf

van der Ploeg, G. R., Westerhuis, J. A., Heintz-Buschart, A., & Smilde, A. K. (2024). *parafac4microbiome: Exploratory analysis of longitudinal microbiome data using Parallel Factor Analysis*. https://doi.org/10.1101/2024.05.02.592191

van der Veen, M. H., Volgenant, C. M. C., Keijser, B., ten Cate, J. (Bob) M., & Crielaard, W. (2016). Dynamics of red fluorescent dental plaque during experimental gingivitis—A cohort study. *Journal of Dentistry*, *48*, 71–76. https://doi.org/10.1016/j.jdent.2016.02.010

Van Der Velden, U., Kuzmanova, D., & Chapple, I. L. C. (2011). Micronutritional approaches to periodontal therapy. *Journal of Clinical Periodontology*, *38*(s11), 142–158. https://doi.org/10.1111/j.1600-051X.2010.01663.x

Van der Weijden, G. A., Timmerman, M. F., Nijboer, A., Lie, M. A., & Van der Velden, U. (1993). A comparative study of electric toothbrushes for the effectiveness of plaque removal in relation to toothbrushing duration: Timerstudy. *Journal of Clinical Periodontology*, *20*(7), 476–481. https://doi.org/10.1111/j.1600-051X.1993.tb00394.x

Volgenant, C. M. C., Zaura, E., Brandt, B. W., Buijs, M. J., Tellez, M., Malik, G., Ismail, A. I., ten Cate, J. M., & van der Veen, M. H. (2017). Red fluorescence of dental plaque in children—A cross-sectional study. *Journal of Dentistry*, *58*, 40–47. https://doi.org/10.1016/j.jdent.2017.01.007

Wemheuer, F., Taylor, J. A., Daniel, R., Johnston, E., Meinicke, P., Thomas, T., & Wemheuer, B. (2020). Tax4Fun2: Prediction of habitat-specific functional profiles and functional redundancy based on 16S rRNA gene sequences. *Environmental Microbiome*, *15*(1), 11. https://doi.org/10.1186/s40793-020-00358-7

WHO. (2022). *Global oral health status report: Towards universal health coverage for oral health by 2030*. WHO. https://www.who.int/publications/i/item/9789240061484

794 Widström, E., Eaton, K., & Vanobbergen, J. (2004). Oral healthcare systems in the Extended European
795 Union, partim:[Oral Health care system in] Belgium. *Oral Health & Preventive Dentistry*, *2*(3),
796 155–157.
797 Zaura, E., Brandt, B. W., Prodan, A., Teixeira de Mattos, M. J., Imangaliyev, S., Kool, J., Buijs, M. J.,
798 Jagers, F. L., Hennequin-Hoenderdos, N. L., Slot, D. E., Nicu, E. A., Lagerweij, M. D., Janus, M.
799 M., Fernandez-Gutierrez, M. M., Levin, E., Krom, B. P., Brand, H. S., Veerman, E. C.,
800 Kleerebezem, M., … Keijser, B. J. (2017). On the ecosystemic network of saliva in healthy young
801 adults. *The ISME Journal*, *11*(5), 1218–1231. https://doi.org/10.1038/ismej.2016.199
802 Zaura, E., Keijser, B. J., Huse, S. M., & Crielaard, W. (2009). Defining the healthy" core microbiome" of
803 oral microbial communities. *BMC Microbiology*, *9*(9).

804
805

806 # Tables

807 *Table 1: Overview of the correlation test results between the time-resolved subject loadings of the PARAFAC models and the*
808 *clinical parameters of gingivitis and microbiome diversity metrics. Red fluorescence was assessed at every time point. Plaque*
809 *and bleeding scores were only assessed at day -14, 0, 14 and 21 of the study. Plaque%: the percentage of sites in the mouth*
810 *that were covered in plaque. Bleeding%: the percentage of sites in the mouth that bled upon probing. RF%: the percentage of*
811 *sites that fluoresced red. Richness: the number of nonzero counts in a sample. Evenness: Shannon diversity divided by*
812 *log(richness). Benjamini-Hochberg corrected p-values of Pearson correlation tests between the subject loadings of one*
813 *component and the clinical parameters are reported (*: p≤0.05; **: p≤0.01; ***: p≤0.001).*

Sample type	Component	Plaque%	Bleeding%	RF%	Richness	Evenness
Upper jaw, lingual	1	0.024*	0.49	8.5e-6***	0.015*	0.032*
	2	0.002**	0.26	4.2e-7***	0.78	1.1e-6***
Upper jaw, interproximal	1	0.0015**	0.032*	8.1e-4***	4.4e-9***	7.0e-9***
	2	0.53	0.15	0.95	0.61	0.94
Lower jaw, lingual	1	4.9e-4***	0.14	1.2e-8***	1.6e-17***	1.5e-12***
Tongue	1	0.78	0.48	0.30	0.024*	0.057
	2	0.85	0.057	0.15	5.3e-11***	0.028*
Saliva	1	0.66	0.20	0.11	0.61	0.78
	2	0.78	0.81	0.78	7.3e-14***	8.5e-6***

814

815

816 *Table 2: Overview of all identified species per ASV cluster. ASVs within the same cluster show a similar response over time to*
817 *the gingivitis intervention. Clustered ASVs are only reported here if two criteria were met: (1) the taxonomic classification was*
818 *resolved to species level by DADA2 using the SILVA (v138) and HOMD (v15.22) databases and (2) the annotation agreed with*
819 *a separate best hit annotation run using the HOMD (v15.22) database. Cases where the classification was resolved to species*
820 *level by the DADA2 run but only to the genus level by the separate HOMD run are also reported.*

Sample type	Cluster	Number of members	Identified species
Upper jaw, lingual	1	9	*Actinomyces naeslundii/oris/viscosus, Kingella oralis, Rothia dentocariosa, Streptococcus cristatis/sinensis, Veillonella dispar/parvula, Veillonella atypica/dispar, Veillonella parvula/rogosae/tobetsuensis*
	2	10	*Fusobacterium canifelinus/nucleatum, Fusobacterium massiliense, Granulicetella elegans, Prevotella nanceiensis, Veillonella massiliensis*
Upper jaw, interproximal	1	3	*Rothia dentocariosa, Veillonella atypica/dispar*
	2	12	*Abiotrophia defectiva, Aggregatibacter aphrophilus/kilianii, Capnocytophaga sputigena, Lachnoanaerobaculum cf., Lautropia mirabilis, Rothia aeria/dentocariosa*
	3	5	*Corynebacterium matruchotii, Leptotrichia hofstaii, Leptotrichia shahii/wadei*
	4	11	*Aggregatibacter segnis, Capnocytophaga granulosa, Capnocytophaga leadberri, Cardiobacterium hominis, Fusobacterium canifelinus/nucelatum, Fusobacterium nucleatum, Leptotrichia buccalis, Porphyromonas pasteri*
Lower jaw, lingual	1	21	*Actinomyces georgiae/pacaensis, Aggregatibacter segnis, Campylobacter concisus, Capnocytophaga granulosa, Capnocytophaga leadbetteri, Cardiobacterium hominis, Corynebacterium matruchotii, Fusobacterium canifelinus/nucleatum, Fusobacterium nucleatum, Fusobacterium hwasooki/nucleatum/periodonticum, Lachnoanaerobaculum cf., Leptotrichia hofstadii, Porphyromonas pasteri*
	2	1	*Streptococcus salivarius* (putative)
Tongue	1	21	*Actinomyces lingnae/marseillensis/pacaensis, Capnocytophaga leadbetteri, Fusobacterium periodonticum, Granulicatella adiacens/para-adiacens, Lachnoanaerobaculum cf., Oribacterium parvum, Oribacterium sinus, Peptostreptococcus stomatis, Porphyromonas pasteri, Prevotella nanceiensis, Veillonella parvula/rogosae/tobetsuensis*
	2	20	*Actinomyces graevenitzii, Alloprevotella rava, Atopobium parvulum, Lachnoanaerobaculum orale/saburreum, Prevotella histicola, Prevotella jejuni/melaninogenica, Prevotella salivae, Prevotella veroralis, Rothia mucilaginosa, Stomatobaculum longum*
Saliva	1	9	*Granulicetella adiacens/para-adiacens, Porphyromonas pasteri, Rothia aeria/dentocariosa*
	2	21	*Actinomyces graevenitzii, Atopobium parvulum, Campylobacter concisus, Lachnoanaerobaculum orale/saburreum, Prevotella histocola, Prevotella jejuni/melanogenica, Prevotella salivae, Rothia mucilaginosa, Stomatobaculum longum, Veillonella atypica/dispar*

821

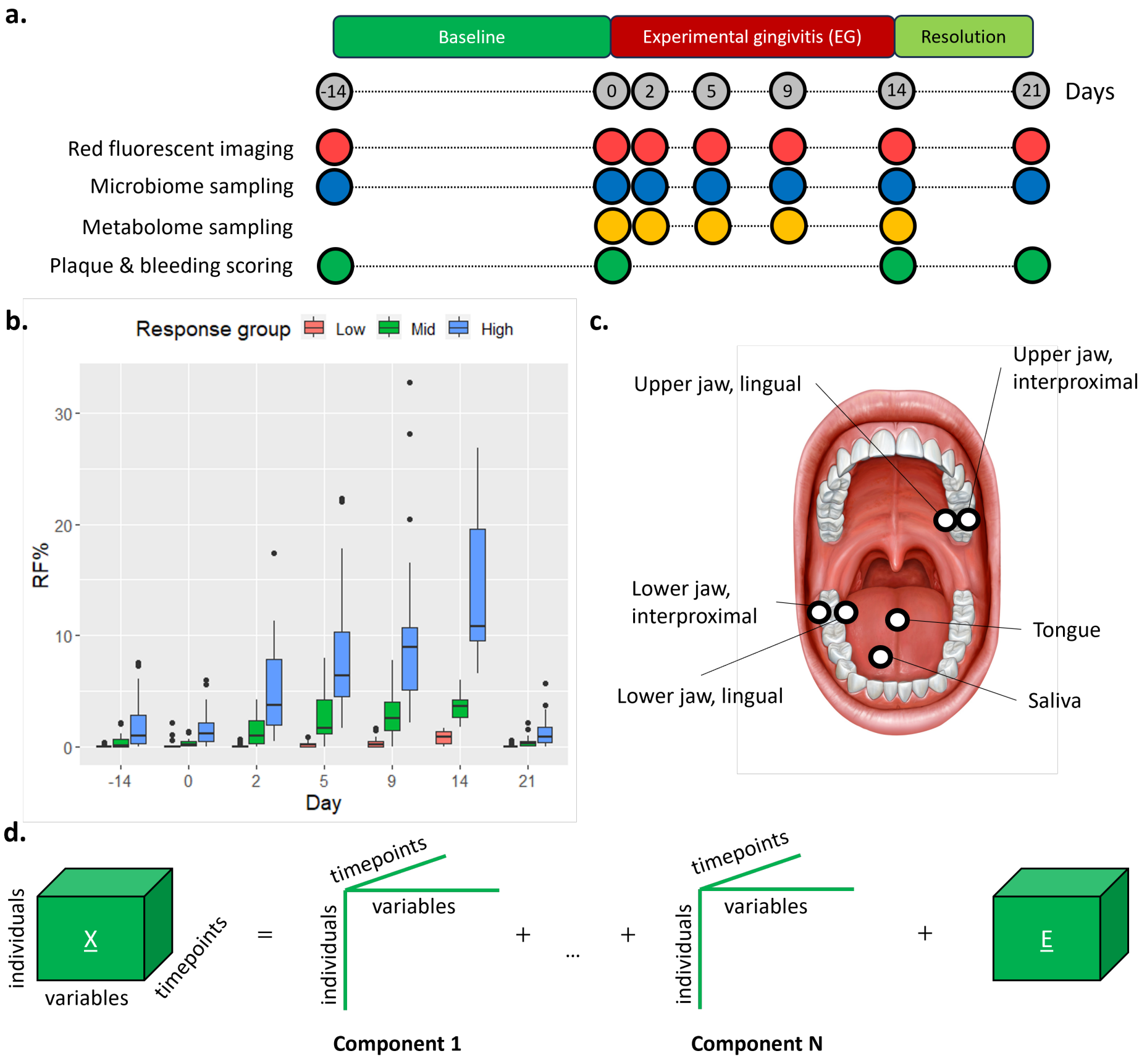
a.
Baseline
Experimental gingivitis (EG)
Resolution
-14
0
2
5
9
14
21
Days
Red fluorescent imaging
Microbiome sampling
Metabolome sampling
Plaque & bleeding scoring
b.
Response group
Low
Mid
High
RF%
30
20
10
0
-14
0
2
5
9
14
21
Day
c.
Upper jaw, lingual
Upper jaw, interproximal
Lower jaw, interproximal
Tongue
Lower jaw, lingual
Saliva
d.
individuals
variables
timepoints
X
=
timepoints
variables
individuals
+
...
+
timepoints
variables
individuals
+
E
Component 1
Component N

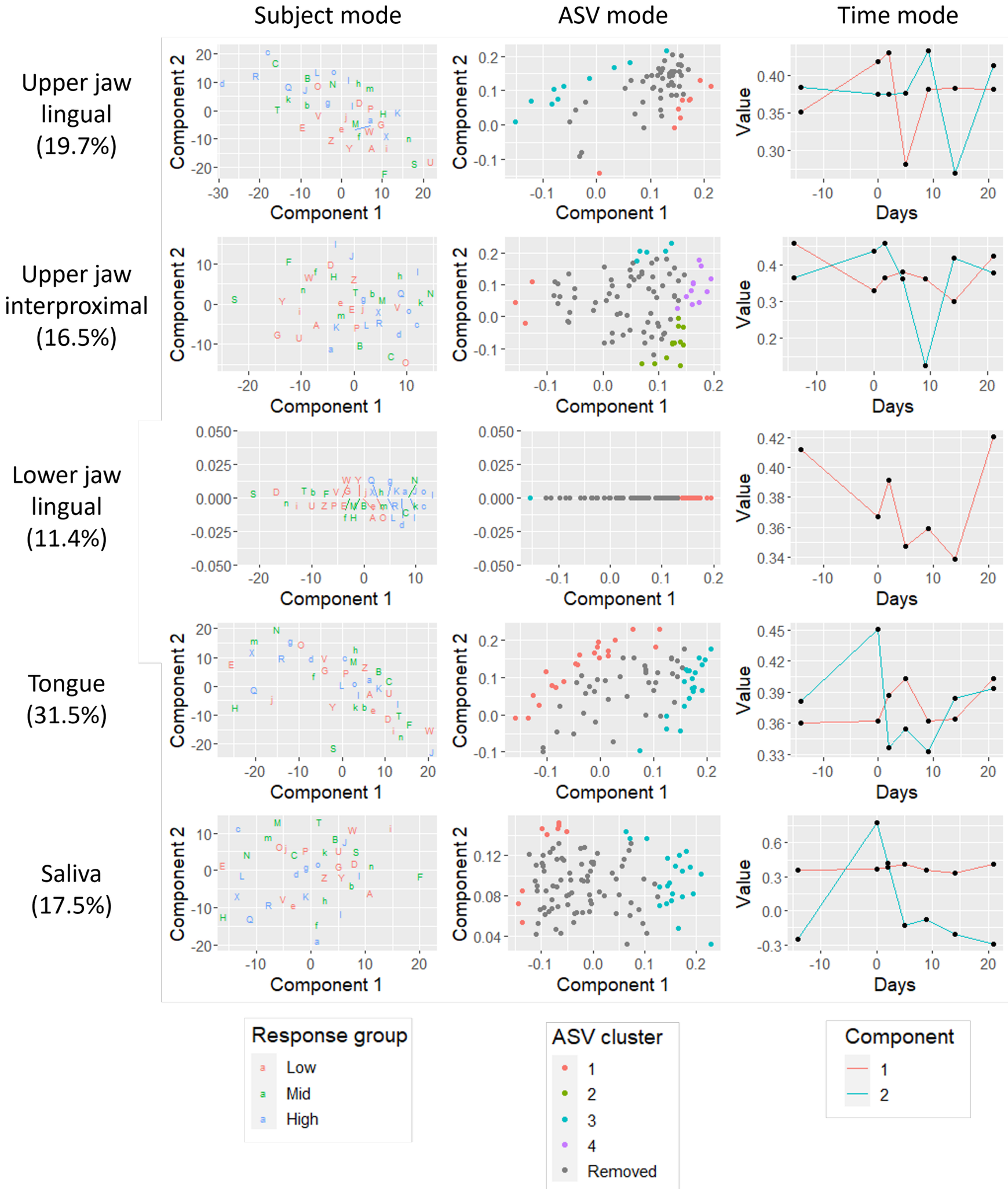
Subject mode
ASV mode
Time mode
Upper jaw lingual (19.7%)
Upper jaw interproximal (16.5%)
Lower jaw lingual (11.4%)
Tongue (31.5%)
Saliva (17.5%)
Component 1
Component 2
Days
Value
Response group
Low
Mid
High
ASV cluster
1
2
3
4
Removed
Component
1
2

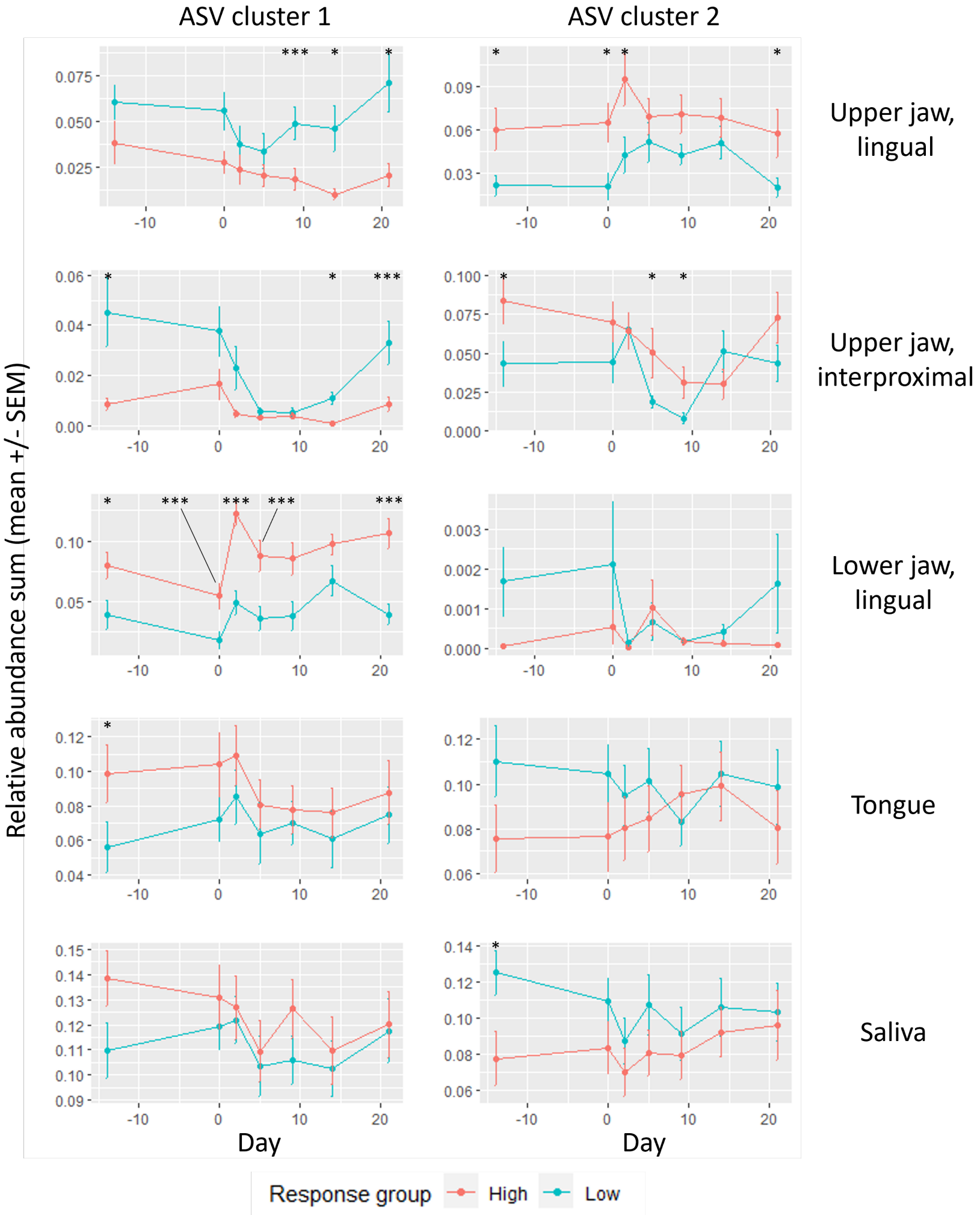
ASV cluster 1
ASV cluster 2
Upper jaw, lingual
Upper jaw, interproximal
Lower jaw, lingual
Tongue
Saliva
Relative abundance sum (mean +/- SEM)
Day
Day
Response group
High
Low

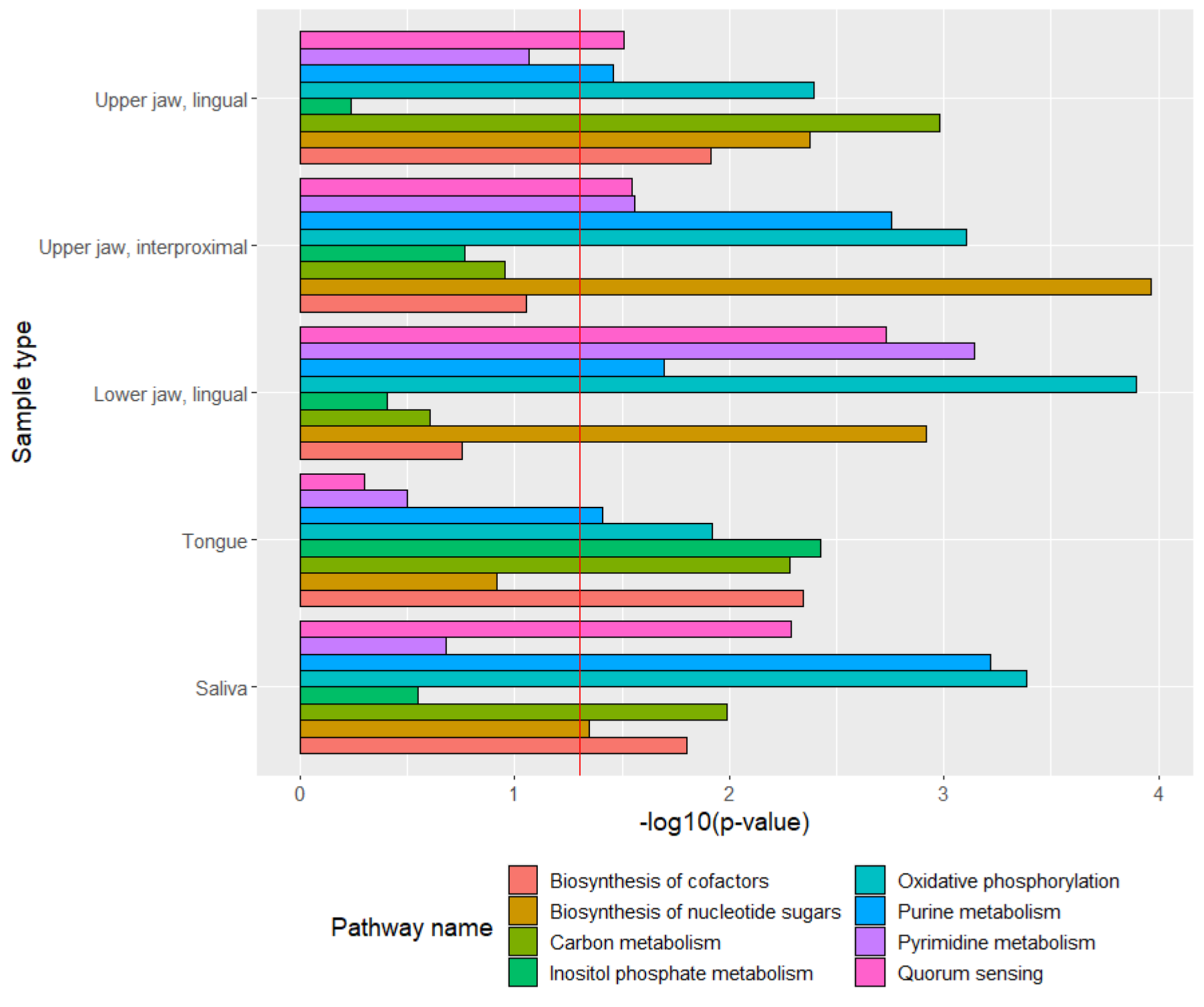
Sample type
Upper jaw, lingual
Upper jaw, interproximal
Lower jaw, lingual
Tongue
Saliva
0
1
2
3
4
-log10(p-value)
Pathway name
Biosynthesis of cofactors
Biosynthesis of nucleotide sugars
Carbon metabolism
Inositol phosphate metabolism
Oxidative phosphorylation
Purine metabolism
Pyrimidine metabolism
Quorum sensing